

AD-A172 223

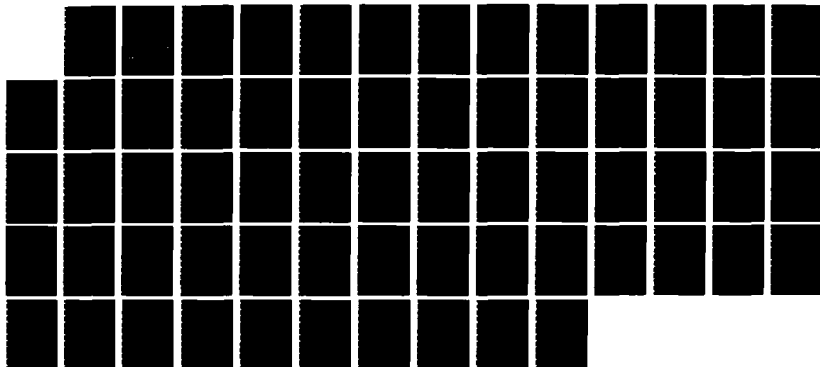
SIGNAL-TO-NOISE RATIO REQUIREMENTS FOR DETECTION OF  
MULTIPLE PULSES SUBJE. (U) NAVAL UNDERWATER SYSTEMS  
CENTER NEW LONDON CT NEW LONDON LAB.

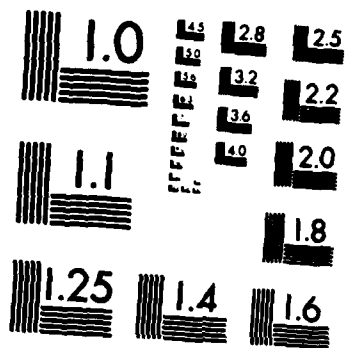
1/1

UNCLASSIFIED

A H NUTTALL ET AL. 82 JUN 86 NUSC-TR-7787 F/G 9/3

NL





MICROCOPY RESOLUTION TEST CHART  
NATIONAL BUREAU OF STANDARDS-1963-A

2

NUSC Technical Report 7707  
2 June 1986

# Signal-to-Noise Ratio Requirements for Detection of Multiple Pulses Subject to Partially Correlated Fading with Chi-Squared Statistics of Various Degrees of Freedom

Albert H. Nuttall  
Edward S. Eby

Surface Ship Sonar Department

AD-A172 223

DTIC FILE COPY

DTIC  
ELECTE  
SEP 23 1986  
S D  
B



**Naval Underwater Systems Center**  
Newport, Rhode Island / New London, Connecticut

Approved for public release, distribution unlimited.

86 9 23 017

## Preface

This research was conducted under NUSC Project No. J20024, "Surface Ship ASW Advanced Development," Principal Investigator Ira B. Cohen (Code 33142), Program Manager David M. Ashworth (Code 33A4), sponsored by Naval Sea Systems Command, Program Element 63553N, Subproject/Task S1704, Program Manager CDR Edward Graham IV (NAVSEA 63D). Also this research was conducted under NUSC Project No. A75205, Subproject No. ZR0000101, "Applications of Statistical Communication Theory to Acoustic Signal Processing," Principal Investigator Dr. Albert H. Nuttall (Code 3314), sponsored by the NUSC In-House Independent Research Program, Program Manager Mr. W. R. Hunt, Director of Navy Laboratories (SPAWAR 05).

The Technical Reviewer for this report was Ira B. Cohen (Code 33142).

Reviewed and Approved: 2 June 1986



W. Von Winkle

Associate Technical Director for Technology

AD- A 172 223

REPORT DOCUMENTATION PAGE				
1a. REPORT SECURITY CLASSIFICATION UNCLASSIFIED		1b. RESTRICTIVE MARKINGS		
2a. SECURITY CLASSIFICATION AUTHORITY		3. DISTRIBUTION / AVAILABILITY OF REPORT Approved for public release; distribution unlimited.		
2b. DECLASSIFICATION / DOWNGRADING SCHEDULE				
4. PERFORMING ORGANIZATION REPORT NUMBER(S) TR 7707		5. MONITORING ORGANIZATION REPORT NUMBER(S)		
6a. NAME OF PERFORMING ORGANIZATION Naval Underwater Systems Center		6b. OFFICE SYMBOL (if applicable)	7a. NAME OF MONITORING ORGANIZATION	
6c. ADDRESS (City, State, and ZIP Code) New London Laboratory New London, CT 06320		7b. ADDRESS (City, State, and ZIP Code)		
8a. NAME OF FUNDING / SPONSORING ORGANIZATION Naval Sea Systems Command		8b. OFFICE SYMBOL (if applicable)	9. PROCUREMENT INSTRUMENT IDENTIFICATION NUMBER	
8c. ADDRESS (City, State, and ZIP Code) Department of the Navy Washington, DC 20362		10. SOURCE OF FUNDING NUMBERS		
		PROGRAM ELEMENT NO.	PROJECT NO. J20024 & A75205	TASK NO.
				WORK UNIT ACCESSION NO.
11. TITLE (Include Security Classification) SIGNAL-TO-NOISE RATIO REQUIREMENTS FOR DETECTION OF MULTIPLE PULSES SUBJECT TO PARTIALLY CORRELATED FADING WITH CHI-SQUARED STATISTICS OF VARIOUS DEGREES OF FREEDOM				
12. PERSONAL AUTHOR(S) Albert H. Nuttall and Edward S. Eby				
13a. TYPE OF REPORT		13b. TIME COVERED FROM TO	14. DATE OF REPORT (Year, Month, Day) 2 June 1986	15. PAGE COUNT
16. SUPPLEMENTARY NOTATION				
17. COSATI CODES			18. SUBJECT TERMS (Continue on reverse if necessary and identify by block number)	
FIELD	GROUP	SUB-GROUP	Signal-to-Noise Ratio Chi-Square Fading	
			Multiple Pulses Diversity Combination	
			Correlated Fading Matched Filters	
19. ABSTRACT (Continue on reverse if necessary and identify by block number)				
<p>The transmitted signal in a fading medium is composed of several pulses separated in time so as to achieve diversity and thereby combat deep fades and loss of signal. Receiver processing consists of matched filtering of each of the pulses, followed by summation of the squared envelopes of all the filter outputs. In addition to additive Gaussian background noise, the signal is subject to slow medium fading which has a chi-squared first-order distribution and which may be correlated from pulse to pulse to an arbitrary degree.</p> <p>The false alarm and detection probabilities of this system are derived in various series expansions which are amenable to efficient computer evaluation. Programs are presented and exercised for various combinations of signal-to-noise ratio, number of pulses, degree of correlated fading, and (noninteger) number of degrees of freedom of the chi-squared fading. Required input signal-to-noise ratios for several false alarm</p>				
20. DISTRIBUTION / AVAILABILITY OF ABSTRACT <input checked="" type="checkbox"/> UNCLASSIFIED/UNLIMITED <input type="checkbox"/> SAME AS RPT <input type="checkbox"/> OTIC USERS			21. ABSTRACT SECURITY CLASSIFICATION UNCLASSIFIED	
22a. NAME OF RESPONSIBLE INDIVIDUAL Albert H. Nuttall			22b. TELEPHONE (Include Area Code) (203) 440-4618	22c. OFFICE SYMBOL Code 3314

18. (Cont'd.)

Detection Probabilities  
 Slow Fading  
 Additive Gaussian Noise  
 Effective Number of Independent Scalings  
 Characteristic Function  
 Exceedence Distribution

19. (Cont'd.)

and detection probabilities are computed and plotted for cases of the fading normalized correlation coefficient ranging from 0 to 1; results for a nonfading medium are superposed for easy comparison.

As special cases of the above formulation, we have independent Rayleigh amplitude fading, as well as completely dependent Rayleigh amplitude fading.

Accession For	
NTIS GRA&I	<input checked="" type="checkbox"/>
DTIC TAB	<input type="checkbox"/>
Unannounced	<input type="checkbox"/>
Justification	
By	
Distribution/	
Availability Codes	
Dist	Avail and/or Special
A-1	

## TABLE OF CONTENTS

	Page
LIST OF ILLUSTRATIONS . . . . .	ii
LIST OF SYMBOLS . . . . .	iii
INTRODUCTION . . . . .	1
PROBLEM DEFINITION . . . . .	5
ANALYTIC RESULTS . . . . .	9
NUMERICAL RESULTS . . . . .	15
SUMMARY . . . . .	29
APPENDICES	
A. CHARACTERISTIC FUNCTION OF SYSTEM OUTPUT . . . . .	31
B. EXCEEDANCE DISTRIBUTION OF SYSTEM OUTPUT . . . . .	41
C. PROGRAM LISTINGS . . . . .	45
REFERENCES . . . . .	51

## LIST OF ILLUSTRATIONS

Figure		Page
1.	Receiver Block Diagram . . . . .	3
2A.	PDF of Normalized Amplitude Scaling . . . . .	16
2B.	PDF of Normalized Power Scaling . . . . .	16
3.	$P_F = 1E-6, P_D = .5, m = 2$ . . . . .	21
4.	$P_F = 1E-6, P_D = .9, m = 2$ . . . . .	21
5.	$P_F = 1E-8, P_D = .5, m = 2$ . . . . .	22
6.	$P_F = 1E-8, P_D = .9, m = 2$ . . . . .	22
7.	$P_F = 1E-6, P_D = .5, m = 1$ . . . . .	23
8.	$P_F = 1E-6, P_D = .9, m = 1$ . . . . .	23
9.	$P_F = 1E-8, P_D = .5, m = 1$ . . . . .	24
10.	$P_F = 1E-8, P_D = .9, m = 1$ . . . . .	24
11.	$P_F = 1E-6, P_D = .5, m = .5$ . . . . .	25
12.	$P_F = 1E-6, P_D = .9, m = .5$ . . . . .	25
13.	$P_F = 1E-8, P_D = .5, m = .5$ . . . . .	26
14.	$P_F = 1E-8, P_D = .9, m = .5$ . . . . .	26
15.	$P_F = 1E-6, P_D = .5, m = .25$ . . . . .	27
16.	$P_F = 1E-6, P_D = .9, m = .25$ . . . . .	27

## LIST OF SYMBOLS

$t$	Time
$L$	Duration of each signal pulse
$f_0$	Carrier frequency
$p(t)$	Pulse waveform, (1)
$\theta_0$	Phase of pulse carrier
$A$	Amplitude of transmitted signal pulse, (2)
$K$	Number of transmitted pulses
$t_k$	Transmission time of $k$ -th pulse
$r_k$	Amplitude scaling due to propagation, (4)
$D$	Bulk delay in propagation
$\tilde{p}$	Randomly phase-shifted signal pulse
$\theta_k$	Random phase shift of $k$ -th pulse
Overbar	Ensemble average
$\overline{E_1}$	Average received signal energy per pulse, (6)
$n(t)$	Additive zero-mean white Gaussian noise
$N_d$	Double-sided noise spectral density level
$N_0$	Single-sided noise spectral density level, $N_0 = 2N_d$
$w(t)$	Received waveform, (7)
$\gamma$	System output; decision variable
$f_\gamma$	Characteristic function of $\gamma$ , (8)
$\xi$	Argument of characteristic function
$\sigma_n^2$	Noise variance, (9)
$\sigma_T^2$	Total variance, (9)

## LIST OF SYMBOLS (Cont'd)

N	Parameter of characteristic function, (10)
R	Signal-to-noise ratio parameter, (9)
$K_e$	Effective number of independent fades, (10)
$\rho_{kl}$	Covariance coefficient of fading, (10),(15)
u	Argument of probability density function
$P_r$	Probability density function of $r_k$
m	Shape parameter in density of $r_k$ , (11)
$\alpha$	Strength parameter in density of $r_k$ , (11)
$q_k$	Power scaling due to propagation, $r_k^2$ , (12)
$\sigma_q$	Standard deviation of $q_k$
$Q_\gamma$	Exceedance distribution function of $\gamma$ , (16)
$P_D$	Probability of detection, (17)
$\lambda$	Normalized threshold, (18)
$e_j(x)$	Partial exponential, (19)
$P_F$	Probability of false alarm, (20)
S	Sum of power scalings, (22)
$E_k$	Received signal energy on k-th pulse for no fading, (23)
$E_T$	Total received signal energy for no fading, (24)
$Q_M(a,b)$	$Q_M$ -function, (28)
PDF	Probability density function
SNR	Signal-to-noise ratio
NF	No fading

## INTRODUCTION

In many situations, the operating environment of an active pulsed system (radar, communications, or sonar) limits the number of pulses transmitted. Moreover the pulses transmitted through a medium, reflected, and returned can be mathematically modeled as received pulses with pulse-to-pulse amplitude variation (fading). An air traffic control radar in a mountainous region operating during severe weather might be subject to such limitations. High frequency radio communication at long ranges (skip distances), when ionospheric conditions are changing because of normal diurnal processes or during solar storms, provide a second class of examples. Replacement of these electromagnetic systems by their acoustic analogues provides the further instance of a sonar operating among islands or at convergence zone ranges (underwater skip distances). The signal-to-noise ratio at the system input could be randomly reduced to a value so low as to preclude acceptable detection performance from processing each signal pulse independently.

Detection performance of a processing system can be mathematically characterized by the parameters  $P_D$ , probability-of-detection, and  $P_F$ , probability-of-false-alarm. When several pulses are transmitted in a pulse train burst, and the returned echoes are processed as a group, we wish to determine the minimum required input signal-to-noise ratio, as a function of the number of pulses,  $K$ , in the burst, necessary to achieve the preassigned acceptable level of performance,  $P_D, P_F$ . Similarly, if only a fixed total

energy is available for transmission, we want to select the "best" distribution of the available energy into  $K$  equal duration pulses to ensure acceptable system performance. Stated differently, what is the optimal number of baskets (pulses) for our eggs (energy)?

For our purposes here, a transmitted burst consists of  $K$  identical, nonoverlapping (in time), sinusoidal pulses. The pulse train received is mathematically modeled as time-delayed, randomly phase-shifted, versions of the transmitted pulses with random pulse-to-pulse amplitude variations of known first-order probability density. This received signal is further corrupted by additive Gaussian white noise. The fading is assumed to be unnoticeably slow during a pulse, so that the only fades it is necessary to model are from pulse-to-pulse, which can be correlated to an arbitrary degree.

One possible detection tactic might be to transmit the smallest energy signal just necessary to achieve the required average detection performance, and accomplish it with a single pulse. Because of a variety of limitations, either physical or financial, this tactic may not achieve the desired performance. Multipulse bursts might work in cases where the available signal-to-noise ratio is low. Here we consider in what sense this intuition is correct for one class of correlated fading, and we compare these results with system performance in a nonfading medium.

In the next section, the characteristics of the transmitted and received signals, the corrupting additive noise, and the receiver processing are

mathematically modeled. This provides notation and scenario for the analysis of the hypothesized receiver, depicted in figure 1. The class of power scaling



Figure 1. Receiver Block Diagram

fading variates considered have chi-square densities so, in a sense, the received envelope amplitude scalings can be thought of as the square roots of chi-square variates. The possibility that several pulses in a pulse train are correlated is covered as well. Numerical examples for several combinations of  $P_D$  and  $P_F$ , for some representative received scaling probability density functions and pulse-to-pulse correlations, are presented and discussed.

Two appendices provide mathematical details supporting the main analysis by deriving the characteristic function and exceedance distribution of the system output; a third appendix lists computer programs for the computation of required input signal-to-noise ratios for fading and nonfading received signals.

TR 7707

## PROBLEM DEFINITION

Signal Characteristics

The detection problem of interest is described in this section. A high-frequency pulse of length  $L$  seconds and carrier  $f_0$  Hz is utilized as the basic signal waveform component:

$$p(t) = \cos(2\pi f_0 t + \theta_0) \quad \text{for } 0 < t < L. \quad (1)$$

We have  $Lf_0 \gg 1$ ; that is, each pulse contains many cycles of the carrier.

The actual transmitted signal waveform is

$$A \sum_{k=1}^K p(t - t_k), \quad (2)$$

where  $A$  is the transmitted signal peak amplitude,  $K$  is the number of pulses, and  $\{t_k\}$  are the transmission times which are arbitrary except that

$$t_{k+1} - t_k > L; \quad \text{i.e., no overlap.} \quad (3)$$

The received signal is

$$A \sum_{k=1}^K r_k \tilde{p}(t - t_k - D), \quad (4)$$

where  $\{r_k\}$  are amplitude scalings imposed by propagation and attenuation through the medium. Bulk delay  $D$  is common to all pulses, and  $\tilde{p}$  denotes a randomly phase-shifted version of (1) by independent uniformly distributed phase shifts  $\{\theta_k\}$  for  $1 \leq k \leq K$ .

The average received signal power during a single pulse is

$$A^2 \overline{r_k^2 \cos^2(2\pi f_0(t - t_k - D) + \theta_0 + \theta_k)} = \frac{1}{2} A^2 \overline{r^2}, \quad (5)$$

and the average received signal energy per pulse is then

$$\overline{E_1} = \frac{1}{2} A^2 \overline{r^2} L. \quad (6)$$

This is a very important parameter regarding the received signal; it is independent of pulse number  $k$  under the assumption that  $\overline{r_k^2} = \overline{r^2}$ , that is, stationary fading.

### Noise Characteristics

There is also assumed present at the receiver input, additive zero-mean white Gaussian noise  $n(t)$  with a double-sided spectrum level  $N_d$  watts/Hz, or equivalently, a single-sided spectrum level  $N_0 = 2N_d$ . The total received waveform is therefore,

$$w(t) = A \sum_{k=1}^K r_k \tilde{p}(t - t_k - D) + n(t). \quad (7)$$

### Receiver Processing

The bulk delay  $D$ , as well as the time separations  $\{t_k\}$  between pulses, are assumed known at the receiver; otherwise, a search over time delay  $D$  is required, in addition to a possible Doppler search, in general. The receiver consists of  $K$  matched filters, one for each of the signal pulses in (4); these filter outputs are envelope detected and sampled at the appropriate instants corresponding to the peak signal outputs. Finally, these envelope samples are squared and summed over the total of  $K$  pulses. This sum is then compared with a threshold for decision about signal presence or absence; see figure 1.

The analytic problem of interest is to determine the probability that the decision variable above exceeds a threshold. From this quantity, we can determine the detection and false alarm probabilities as functions of all the various parameters presented in (1) - (7). Then for specified detection and false alarm probabilities, the required input signal-to-noise ratio,  $\bar{E}_1/N_0$ , can be determined numerically.

TR 7707

## ANALYTIC RESULTS

Characteristic Function of Decision Variable

The derivations of the statistics of the decision variable  $\gamma$  are conducted in appendices A and B. Specifically, the characteristic function of  $\gamma$  is given in (A-31) as

$$f_{\gamma}(s) = \left(1 - i\sqrt{2}\sigma_n^2 s\right)^{N-K} \left(1 - i\sqrt{2}\sigma_T^2 s\right)^{-N}, \quad (8)$$

where

$$\sigma_n^2 = \frac{1}{4} N_0 L, \quad \sigma_T^2 = \sigma_n^2 (1 + R), \quad R = \frac{\overline{E}_1}{N_0} \frac{K}{N},$$

$$\frac{\overline{E}_1}{N_0} = \frac{\text{average received signal energy per pulse}}{\text{single-sided received noise spectral density level}}, \quad (9)$$

and

$$N = m K_e, \quad K_e = \frac{K^2}{\sum_{k,l=1}^K \rho_{kl}}. \quad (10)$$

Here,  $m$  is a parameter in the first order probability density function of amplitude scalings  $\{r_k\}$ , namely,

$$p_r(u) = \frac{2 u^{2m-1} \exp(-u^2/\alpha)}{\Gamma(m) \alpha^m} \quad \text{for } u > 0 \quad (m > 0). \quad (11)$$

To explain the other parameters in (10), we use the power scaling variable

$$q_k = r_k^2 \quad (12)$$

for the k-th pulse in (4) and (7). From (11), the probability density function of  $\{q_k\}$  is

$$p_q(u) = \frac{u^{m-1} \exp(-u/\alpha)}{\Gamma(m) \alpha^m} \quad \text{for } u > 0 \quad (m > 0) . \quad (13)$$

This is recognized as a chi-squared variate of  $2m$  degrees of freedom; however,  $2m$  need not be an integer. It is readily verified that

$$\frac{\text{Std Dev}(q)}{\text{Mean}(q)} = \frac{\sigma_q}{\bar{q}} = \frac{1}{\sqrt{m}} . \quad (14)$$

Thus as  $m \rightarrow \infty$ , the probability density function of power scaling  $q_k$  narrows about its mean value,\* while if  $m \rightarrow 0$ , it develops a large cusp at the origin and a significant spread about the mean.

The normalized covariance coefficient appearing in (10) is that of the power scaling variates:

$$\rho_{k\ell} = \frac{1}{\sigma_q^2} \overline{(q_k - \bar{q})(q_\ell - \bar{q})} . \quad (15)$$

It measures the degree of correlation between the fading imposed on the signal pulses, i.e.,  $\{r_k\}$  in (7).

---

\*This corresponds to a nonfading medium.

The quantity  $K_e$  in (10) can be interpreted as an effective number of independent scalings in (4) and (7). For example, if  $\rho_{k\ell} = 0$  for  $k \neq \ell$ , then  $K_e = K$ ; while if  $\rho_{k\ell} = 1$  for all  $k, \ell$ , then  $K_e = 1$ . Both of these situations agree with physical intuition. No specific time separations  $\{t_k\}$ , in (4) and (7), need be assumed for (10) to apply; some of the pulses can be close together, while others can be widely separated, subject of course to limitation (3). The only way that the statistical dependencies of the power scalings  $\{q_k\}$  enter the characteristic function of  $\gamma$  is through the double summation of covariance coefficients in (10).

However, it must be remarked that the result in (8) is only an approximation, developed in appendix A. An exact analysis of the characteristic function of output  $\gamma$  is the subject of a future study.

#### Exceedance Distribution Function of Decision Variable

Three alternative forms for the exceedance distribution function of  $\gamma$ ,

$$Q_\gamma(u) = \text{Prob}(\gamma > u) , \quad (16)$$

are developed in appendix B, namely, (B-9), (B-11), and (B-13), each having different merits, as discussed there. The one we have used for our numerical calculations is the last one, and is, in fact, the detection probability when signal is present:

$$P_D = 1 - \frac{\exp(-\lambda)}{(1+R)^N} \sum_{n=0}^{\infty} \frac{\binom{N}{n}}{n!} \left(\frac{R}{1+R}\right)^n \left[ \exp(\lambda) - e_{K-1+n}(\lambda) \right]. \quad (17)$$

Here

$$\lambda = \frac{u}{2\sigma_n^2} \quad (18)$$

is a normalized threshold, and

$$e_j(x) = \sum_{n=0}^j x^n/n! \quad (19)$$

is the partial exponential [1; 6.5.11]. The other two parameters appearing in  $P_D$ , namely,  $R$  and  $N$ , have already been explained in (9) and (10).

The false alarm probability corresponding to (17) is obtained by setting  $R = 0$ :

$$P_F = \exp(-\lambda) e_{K-1}(\lambda). \quad (20)$$

Thus, the performance of the diversity combining processor is governed by the fundamental pair of equations, (17) and (20). For a specified number of pulses  $K$  and false alarm probability  $P_F$ , (20) can be solved for threshold  $\lambda$ . These values of  $K$  and  $\lambda$  are then employed in (17) to evaluate detection probability  $P_D$  for any specified  $N$  and  $\bar{E}_1/N_0$ . A program for this procedure is given in appendix C.

Detection Probability for Nonfading Medium

For comparison purposes, the detection probability for the processor of figure 1 in the presence of a deterministic, i.e., nonfading, medium is also presented. This result is most easily obtained from the conditional characteristic function for the system output, as presented in (A-13) and (A-14):

$$f_Y^{(c)}(\xi) = \left(1 - i\xi 2\sigma_n^2\right)^{-K} \exp\left[\frac{i\xi}{1 - i\xi 2\sigma_n^2} \left(\frac{AL}{2}\right)^2 S\right], \quad (21)$$

where

$$S = \sum_{k=1}^K q_k. \quad (22)$$

is the sum of the power scalings on all K pulses. Since there is no fading, (21) is directly the characteristic function of the decision variable.

A more convenient form for (21) is available when we observe from (4) and (1) that the received signal energy on the k-th pulse is the nonrandom quantity

$$E_k = A^2 r_k^2 \frac{1}{2} L = \frac{1}{2} A^2 L q_k. \quad (23)$$

Thus, the total received signal energy is, using (22),

$$E_T = \sum_{k=1}^K E_k = \frac{1}{2} A^2 L S. \quad (24)$$

Coupled with the expression for  $\sigma_n^2$  given in (9), we obtain for (21), the characteristic function,

$$f_Y^{(c)}(\xi) = \left(1 - i\xi 2\sigma_n^2\right)^{-K} \exp \left[ \frac{i\xi 2\sigma_n^2}{1 - i\xi 2\sigma_n^2} \frac{E_T}{N_0} \right], \quad (25)$$

in terms of the parameter

$$\frac{E_T}{N_0} = \frac{\text{total received signal energy over } K \text{ pulses}}{\text{single-sided received noise spectral density level}}. \quad (26)$$

The exceedance distribution function corresponding to (25) is available from [2; (50) and (51)] as

$$P_D = Q_K \left( \left( \frac{2E_T}{N_0} \right)^{1/2}, (2\lambda)^{1/2} \right), \quad (27)$$

where we used (18) and the  $Q_M$ -function defined as

$$Q_M(a, b) = \int_b^\infty dx \, x \left( \frac{x}{a} \right)^{M-1} \exp \left( -\frac{x^2 + a^2}{2} \right) I_{M-1}(ax). \quad (28)$$

The false alarm probability corresponding to (27) is obtained by setting  $E_T = 0$ , and is identically (20), as it must be, since the background noise is independent of any signal fading characteristics.

When we plot these latter results for a nonfading medium, and compare them with the earlier results in (17) for the fading medium of interest, we replace  $E_T$  by  $K \bar{E}_1$ . This arbitrary but reasonable assignment is necessary in order to superpose the two types of results on one plot. However, strictly speaking, the parameter  $\bar{E}_1/N_0$  appearing in the following plots should be interpreted as  $E_T/(KN_0)$  in the case of no fading.

## NUMERICAL RESULTS

The probability density functions (PDF) for five values of the scaling parameter  $m$  in (11) and (13), representing five distinct possible fading behaviors, are plotted in figure 2. All densities of the class considered vanish for negative argument. So these behaviors are, for the amplitude variate: (1) an impulse representing the nonfading case, which is also the limiting case of the class as  $m \rightarrow \infty$ ; (2) continuous with continuous derivative at the origin ( $m = 2$ ); (3) continuous with discontinuous derivative at the origin ( $m = 1$ , Rayleigh amplitude density); (4) a finite discontinuity at the origin ( $m = 1/2$ , a one-sided or full-wave rectified zero-mean Gaussian density); and (5) an infinite cusp at the origin ( $m = 1/4$ ). The amplitude scaling  $r$ , with the probability density function of (11), has second moment

$$\overline{r^2} = m\alpha. \quad (29)$$

The normalized amplitude scaling

$$\hat{r} = r / (\overline{r^2})^{1/2}, \quad (30)$$

normalized by the root-mean-square (rms) value of the amplitude scaling (not the standard deviation  $\sigma_r$ ), has probability density function

$$p_{\hat{r}}(u) = \frac{2 m^m u^{2m-1} \exp(-mu^2)}{\Gamma(m)} \quad \text{for } u > 0. \quad (31)$$

For the five values of  $m$  ( $=\infty, 2, 1, 1/2, 1/4$ ), the probability density functions for this rms-normalized amplitude scaling are shown in figure 2A.

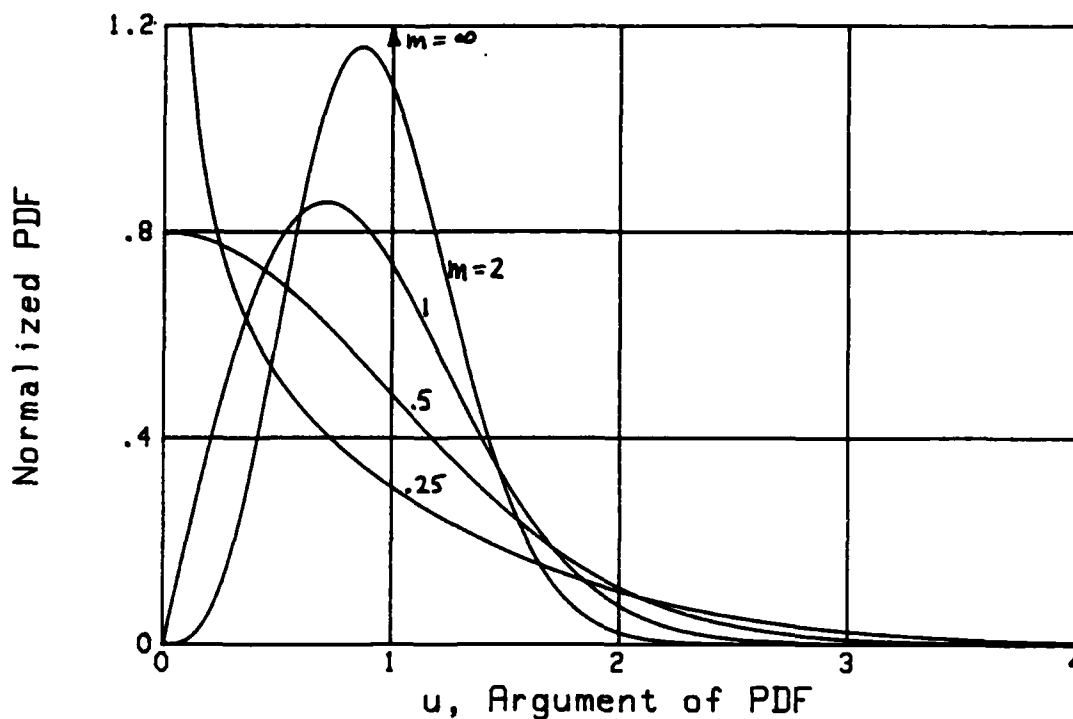


Figure 2A. PDF of Normalized Amplitude Scaling

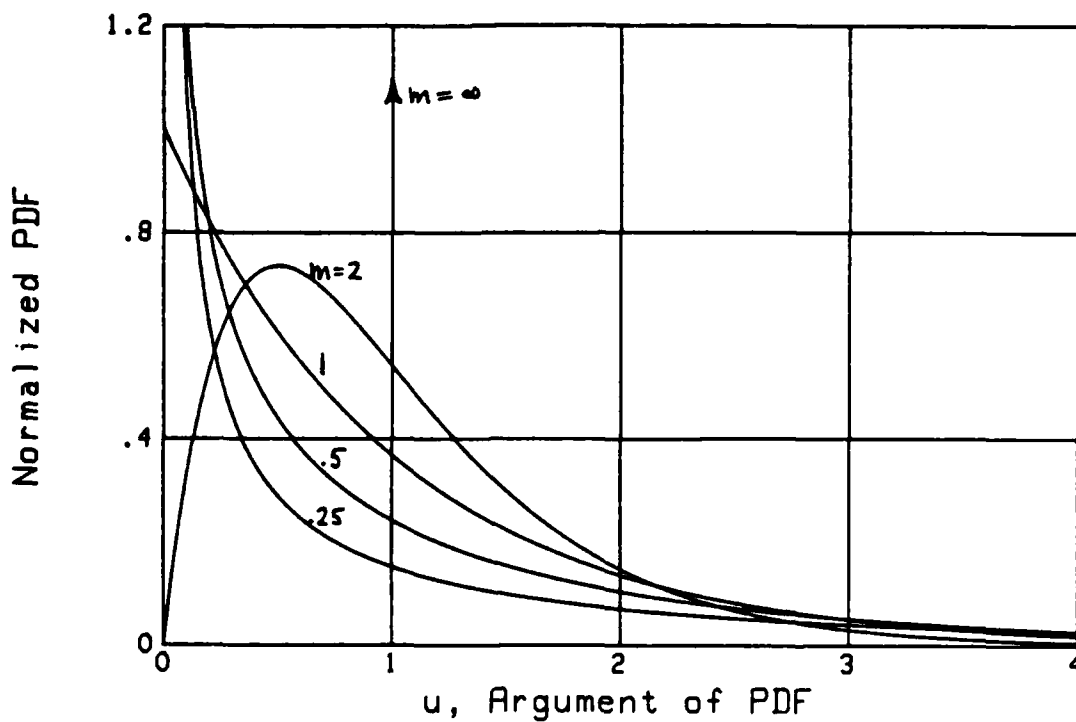


Figure 2B. PDF of Normalized Power Scaling

The corresponding probability density functions for power scaling  $q$  are chi-squared variates with  $2m$  degrees of freedom, as given in (13). The mean of variate  $q$  is

$$\bar{q} = m\alpha. \quad (32)$$

The normalized power scaling

$$\tilde{q} = q/\bar{q}, \quad (33)$$

normalized by the mean power, has probability density function

$$p_{\tilde{q}}(u) = \frac{m^m u^{m-1} \exp(-mu)}{\Gamma(m)} \quad \text{for } u > 0. \quad (34)$$

The normalized power scaling probability density functions are plotted in figure 2B for the same five values of  $m$ .

For each finite value of  $m$  above, and for each of the four combinations of system performance parameters  $P_D = .5$  or  $.9$ , and  $P_F = 1E-6$  or  $1E-8$ , the required minimum system input signal-to-noise ratio (SNR) to achieve this performance, as a function of the number of pulses  $K$  in a pulse train, has been computed using the computer programs listed in appendix C which implement the theoretical analysis above. Although this analysis and these programs can handle general pulse-to-pulse normalized covariance coefficients  $\{\rho_{kl}\}$ , the figures have been computed for the special case of exponential correlation

$$\rho_{kl} = \rho^{|k-l|}, \quad -1 \leq \rho \leq 1. \quad (35)$$

Each of the graphs has two sets of curves: the solid curves are for the required average received signal energy per pulse ( $\bar{E}_1/N_0$ ) in dB, as a function of the number of pulses  $K$ , and the dotted curves are for the total average received signal energy ( $\bar{E}_T/N_0$ ) in dB. For ease of comparison, each set of curves on each graph includes its nonfading (NF) or  $m \rightarrow \infty$  counterpart. In every case computed, the solid curves show that the energy per pulse, or input signal-to-noise ratio required for acceptable system performance, decreases as the number of pulses increases. This matches the intuitive argument that using more pulses implies we are using more total energy, so we should be able to maintain the same level of performance with less energy per pulse. The intuitive conclusion is correct, but scanning the dotted sets of curves (representing total energy in the pulse train) shows this intuitive argument is only part of the story. For more-or-less uncorrelated adjacent pulse fading and for the smaller scaling parameters ( $m \leq 1$ ), the total input signal energy required initially decreases as we increase the number of pulses in a pulse train. For a large number of pulses, the total energy will eventually increase with  $K$ , but for a small number of pulses, a short burst may be more efficient. For example, with  $P_D = .5$ ,  $P_F = 1E-8$ , and a one-sided Gaussian amplitude probability density function,  $m = 1/2$ , figure 13 shows that the total energy required reaches a minimum of 14.4 dB for  $\rho = 0$  with 3 pulses per burst; for  $\rho = .5$ , the minimum of 15.2 dB occurs with 5 pulses. In all cases, the  $\rho = .5$  curve is closer to the  $\rho = 0$  curve than to the  $\rho = 1$  curve, and the high correlation  $\rho = 1$  curve always increases. Thus, for moderate values of correlation, we can expect system performance to be robust and system performance will be severely degraded only for highly correlated fading.

As the exponential covariance coefficient  $\rho$  in (35) decreases toward  $-1$ , the performance curves for even  $K$  approach those corresponding to the nonfading case. This is easily seen since the sum of two successive power scalings in the sum  $S$  in (22) and (A-14) then tends to  $2\bar{q}$ , twice the mean of  $q$ , which is a nonrandom quantity. Equivalently, we can say the random fluctuations in the power scalings  $\{q_k\}$  have canceled each other. For  $K$  odd, however, there is always one unpaired random fluctuation, even for  $\rho = -1$ ; this means that for  $K$  odd and  $\rho = -1$ , system performance is slightly poorer than for the nonfading situation. As  $K$  increases through odd values, this discrepancy decreases to insignificance. Even for  $K = 3$ , the difference is small. This has been confirmed analytically and verified by numerical calculation for values of  $\rho$  very near  $-1$ , and for several  $K$ ; these results have been omitted from the figures which include only nonnegative values of  $\rho$ .

A separate issue is whether values of  $\rho$  near  $\rho = -1$  can be realized. That is, if the first-order probability density function of the nonnegative power scaling variate  $q$  is not symmetric about its mean  $\bar{q}$ , then arbitrarily large negative values of  $\rho$  are not allowed. For example, for  $\rho_{k\ell}$  to reach  $-1$ , we would need  $(q_k - \bar{q}) = -(q_\ell - \bar{q})$  with probability one. However, for the class of power scalings treated here, this is clearly impossible: large positive values of  $q_k - \bar{q}$  occur with nonzero probability, for which the corresponding negative values  $-(q_k - \bar{q})$  occur with probability zero. Thus, for most probability density functions, and in particular for the class assumed here, the  $\rho = -1$  results would represent an unreachable bound to

system performance. This is an illustration of the fact that the first-order probability density function and the correlation (or spectrum) of a random process cannot be independently specified in general. Complete first-order information imposes some restrictions on allowable second-order statistics.

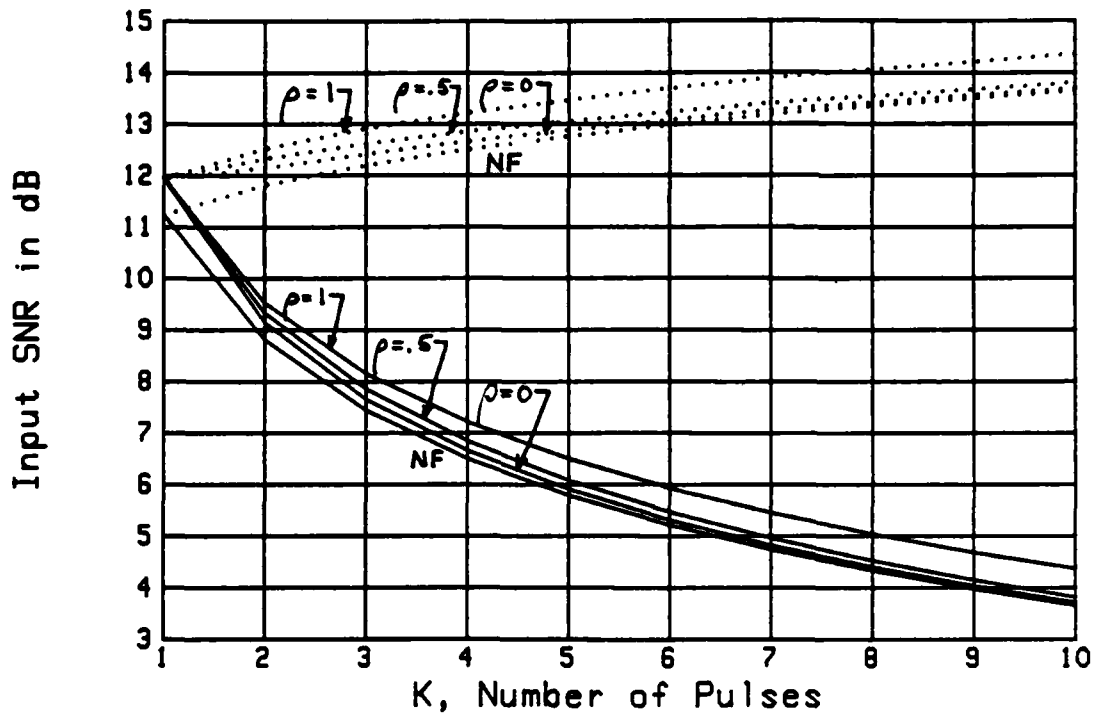


Figure 3.  $P_f = 1E-6$ ,  $P_b = .5$ ,  $m = 2$

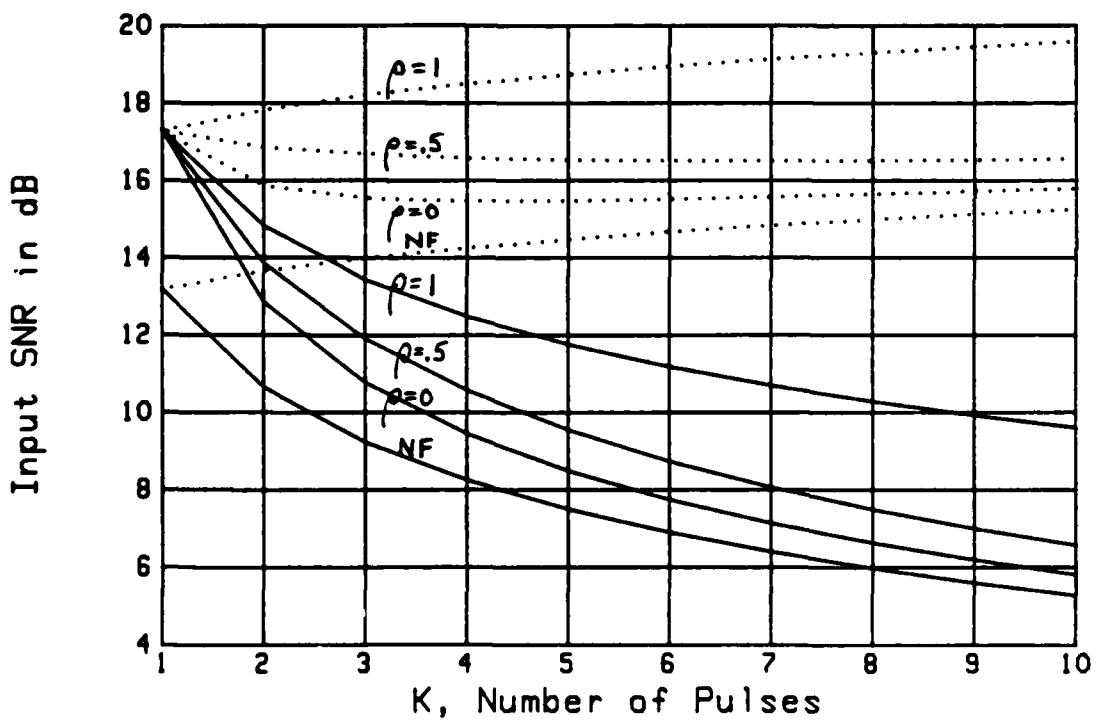


Figure 4.  $P_f = 1E-6$ ,  $P_b = .9$ ,  $m = 2$

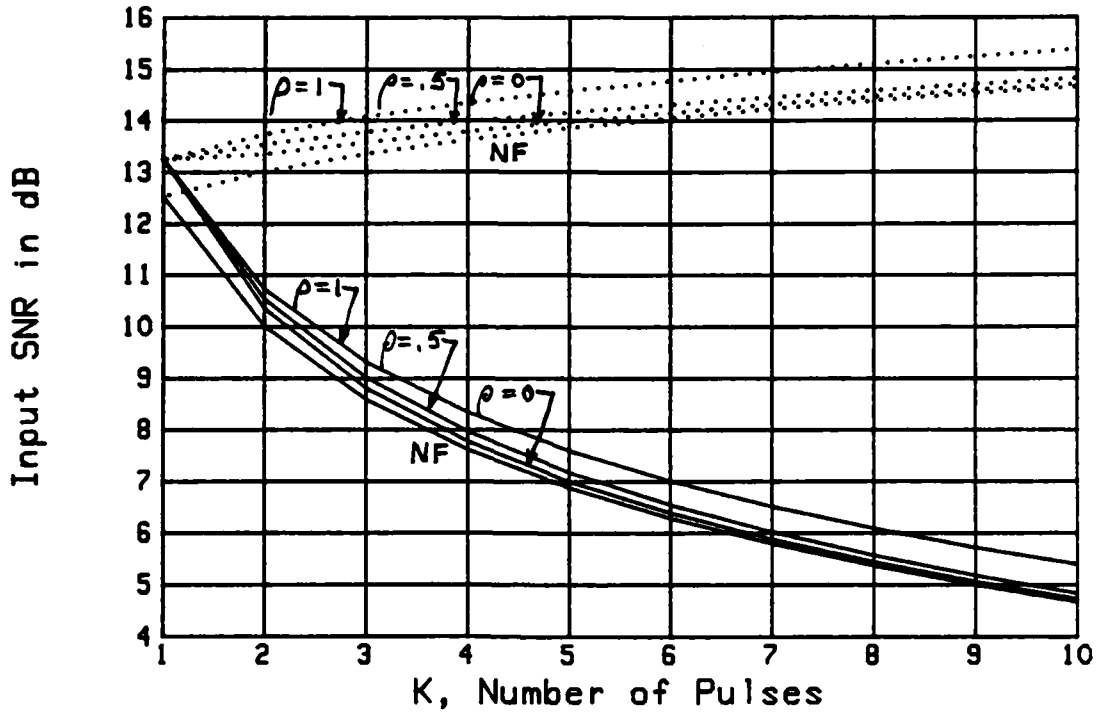


Figure 5.  $P_f = 1E-8$ ,  $P_d = .5$ ,  $m = 2$

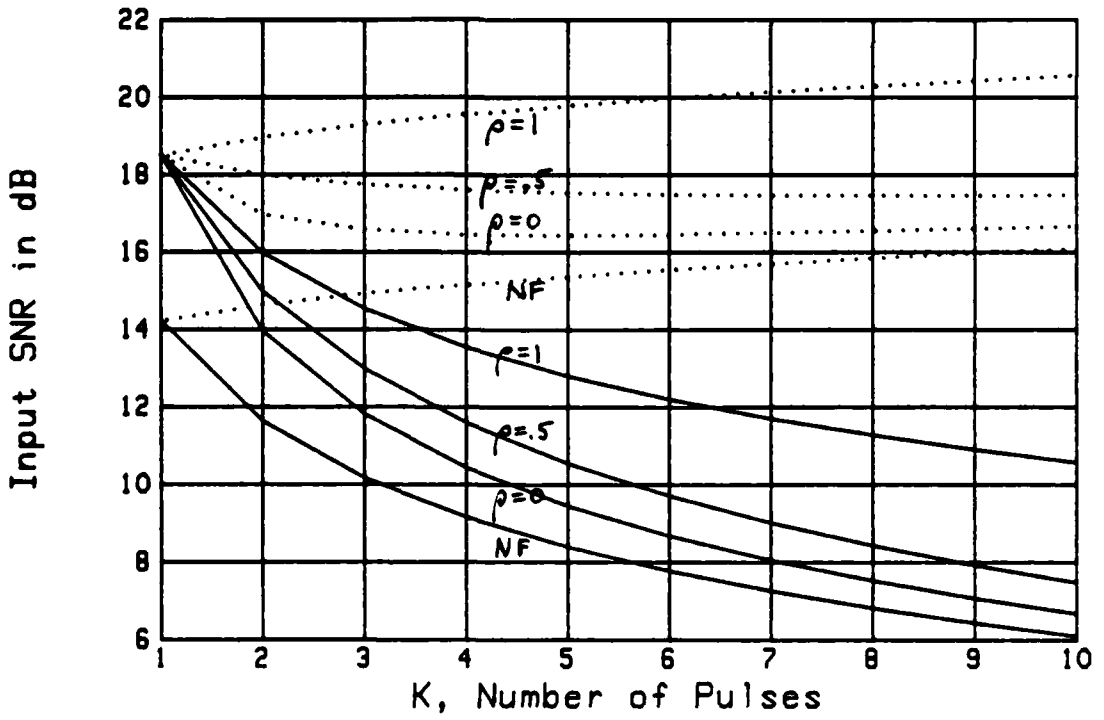


Figure 6.  $P_f = 1E-8$ ,  $P_d = .9$ ,  $m = 2$

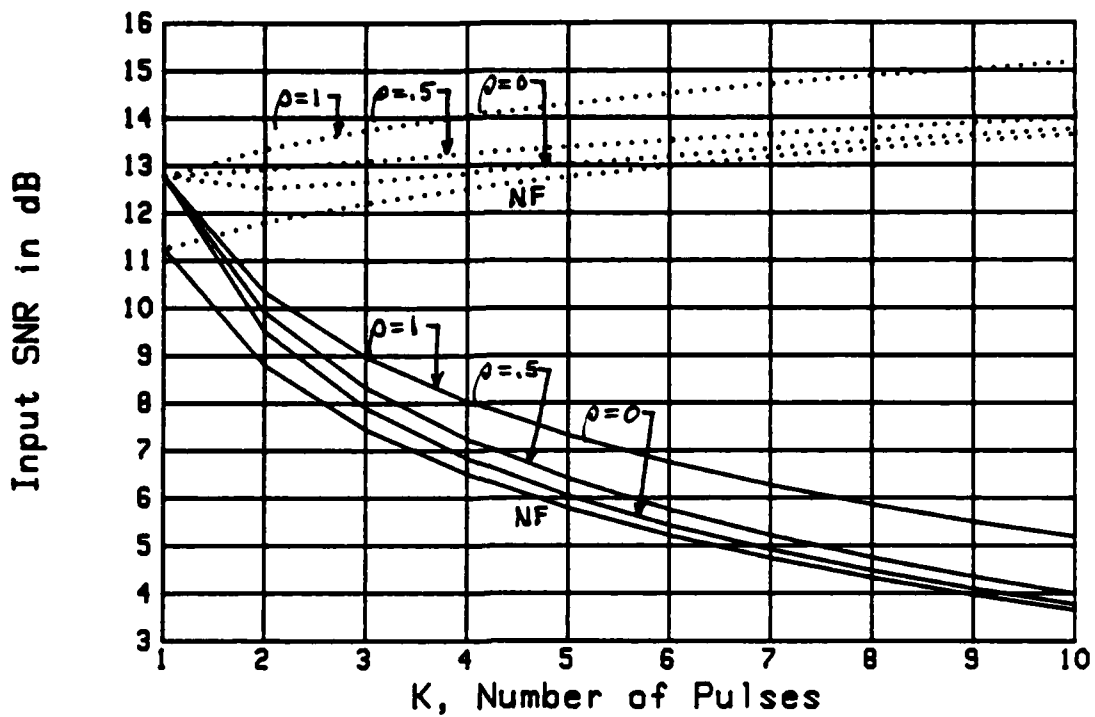


Figure 7.  $P_f = 1E-6$ ,  $P_b = .5$ ,  $m = 1$

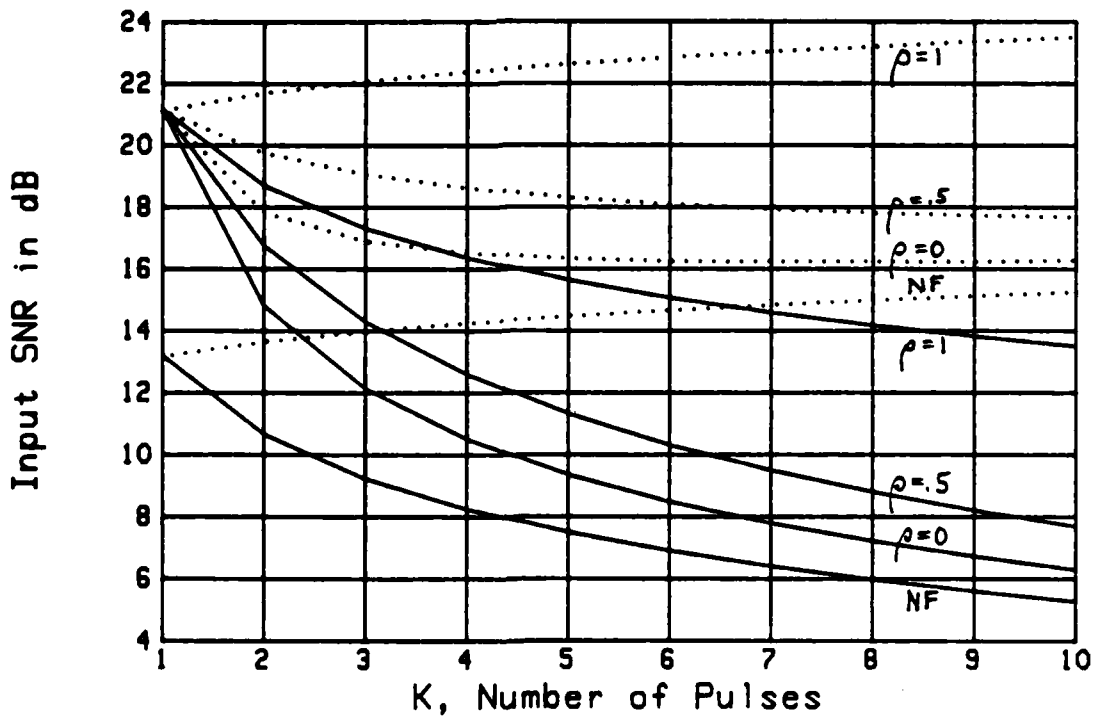


Figure 8.  $P_f = 1E-6$ ,  $P_b = .9$ ,  $m = 1$

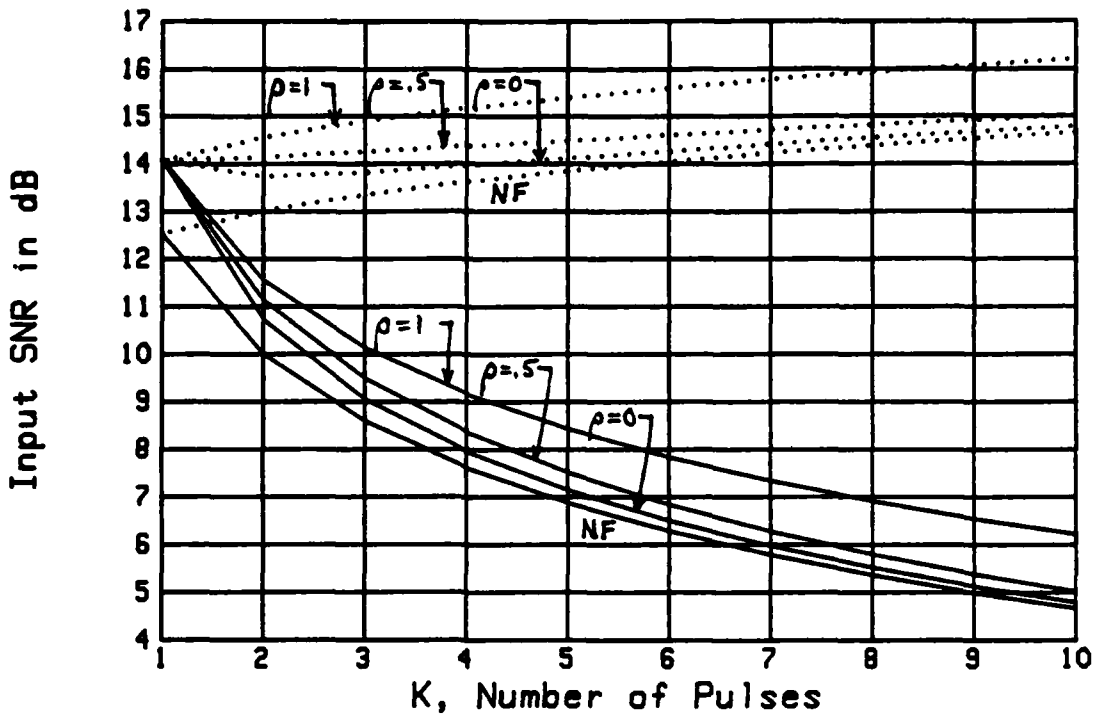


Figure 9.  $P_F = 1E-8$ ,  $P_D = .5$ ,  $m = 1$

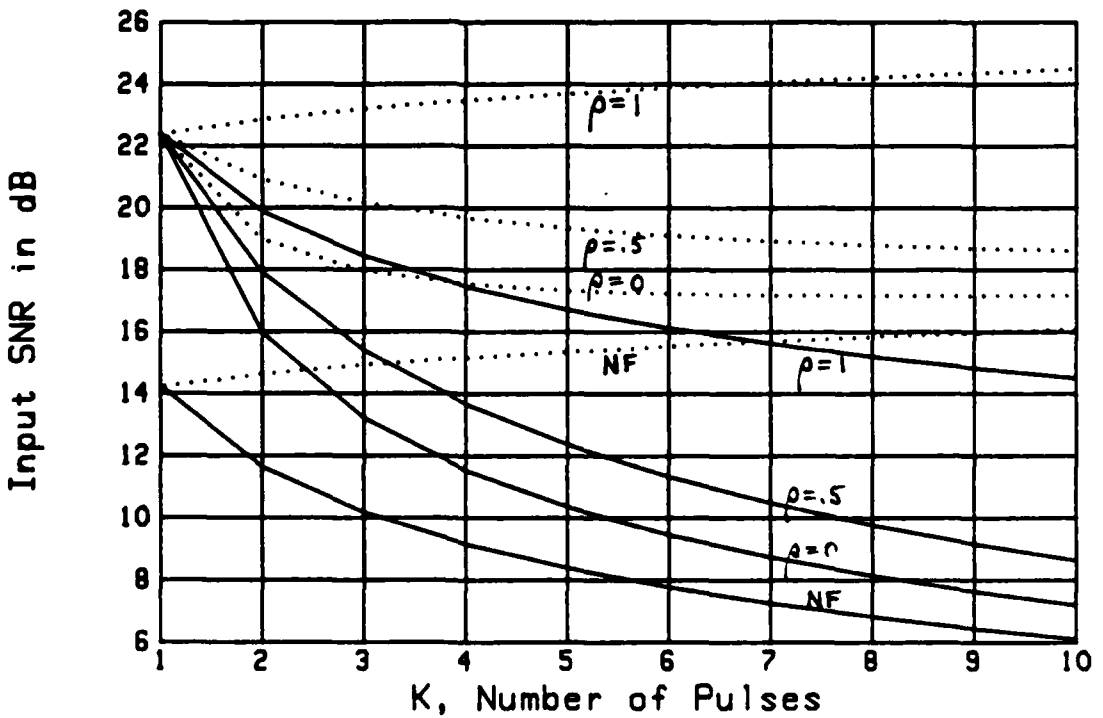


Figure 10.  $P_F = 1E-8$ ,  $P_D = .9$ ,  $m = 1$

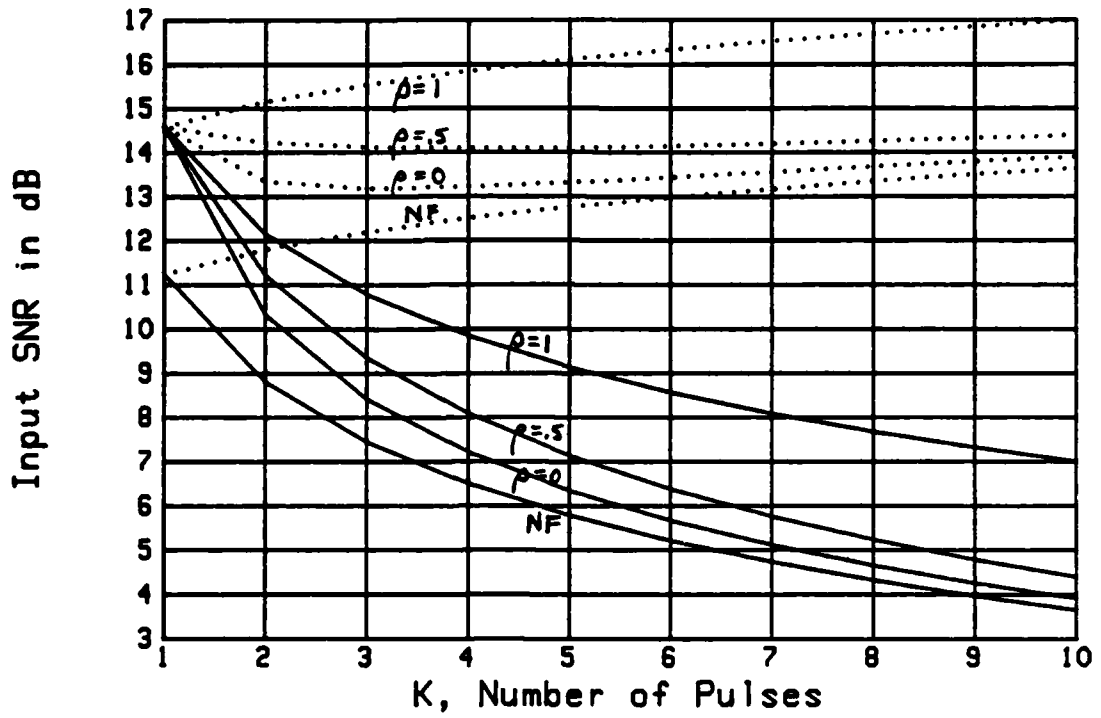


Figure 11.  $P_f = 1E-6$ ,  $P_b = .5$ ,  $m = .5$

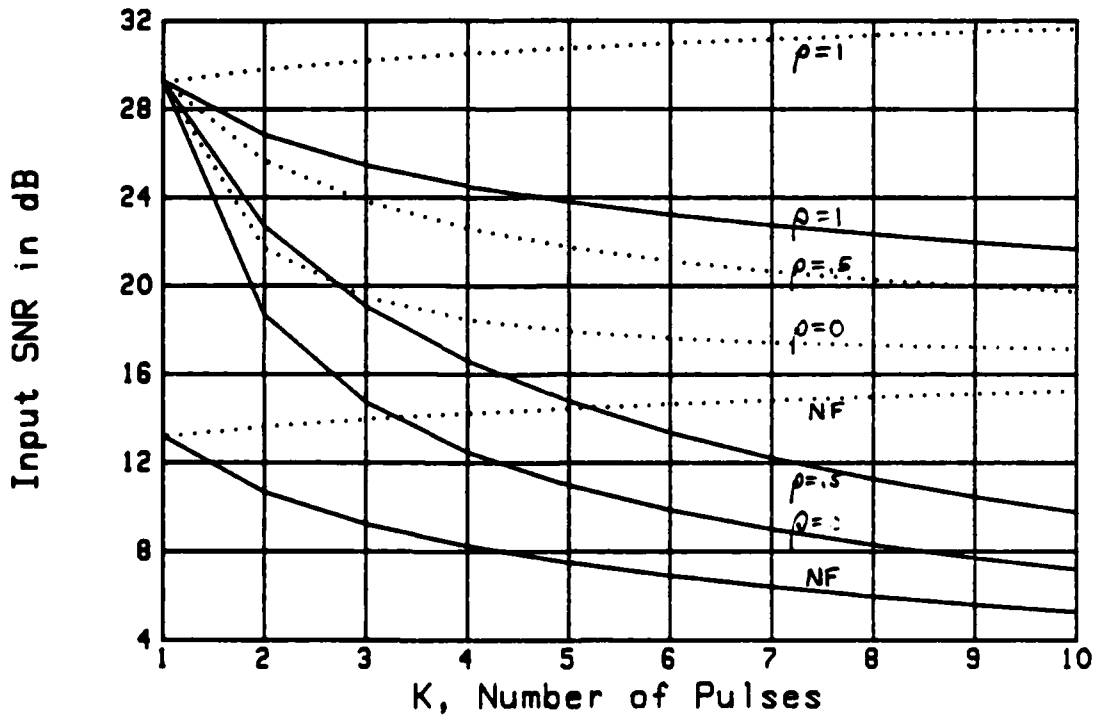


Figure 12.  $P_f = 1E-6$ ,  $P_b = .9$ ,  $m = .5$

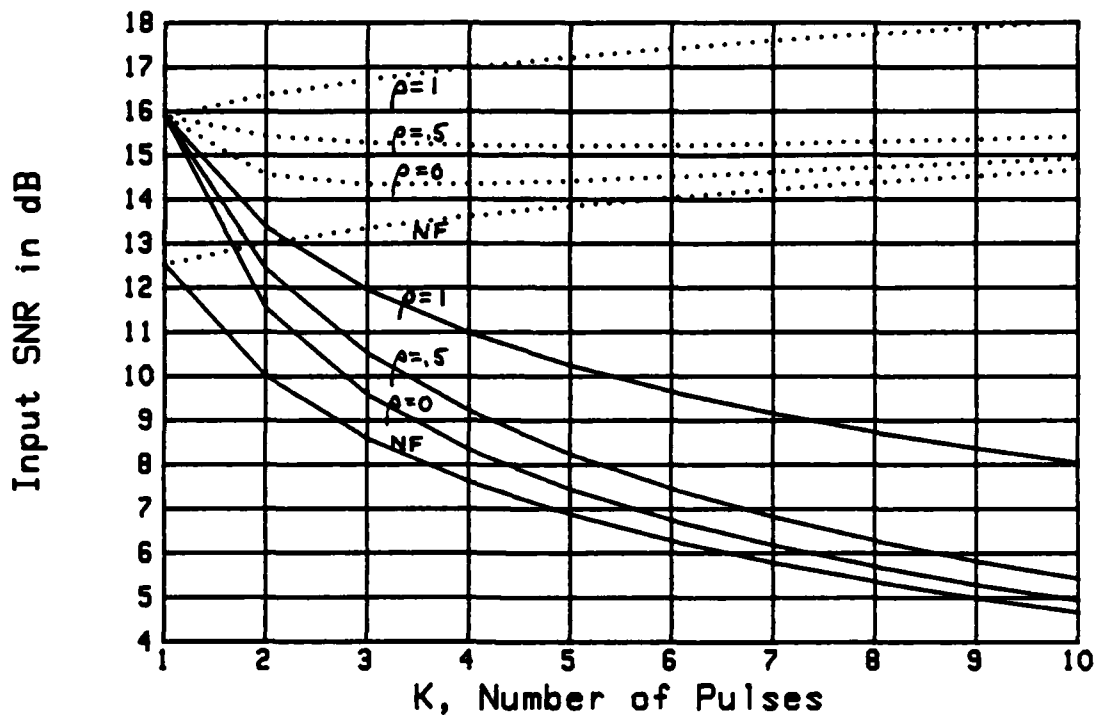


Figure 13.  $P_F = 1E-8$ ,  $P_D = .5$ ,  $m = .5$

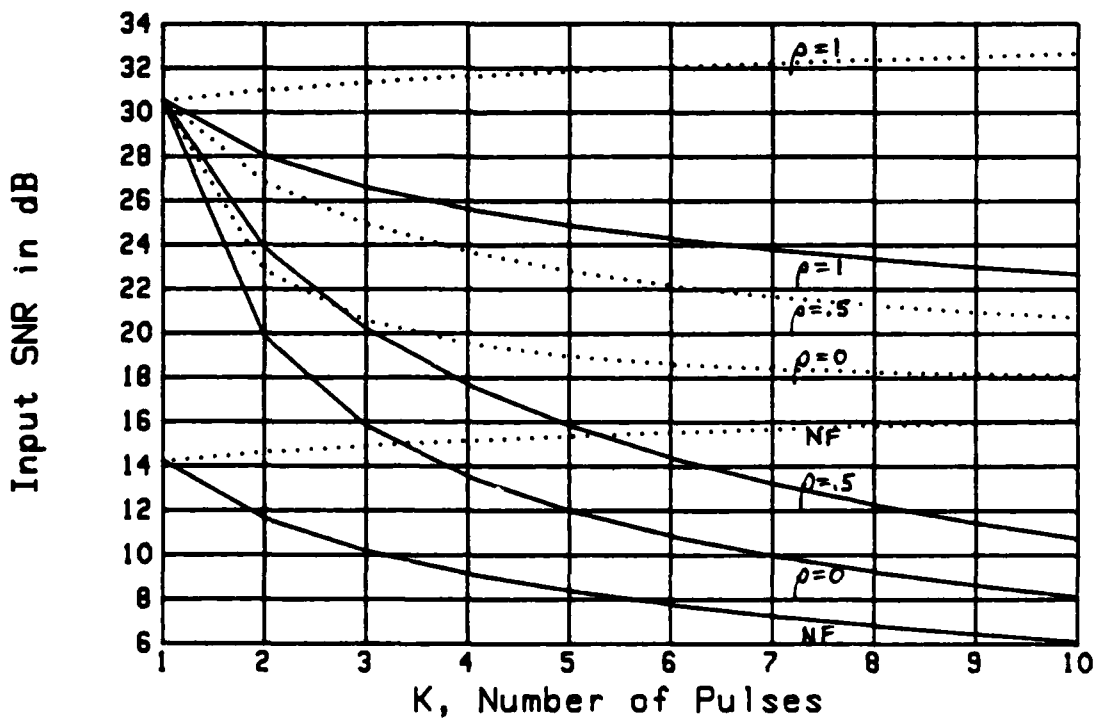


Figure 14.  $P_F = 1E-8$ ,  $P_D = .9$ ,  $m = .5$

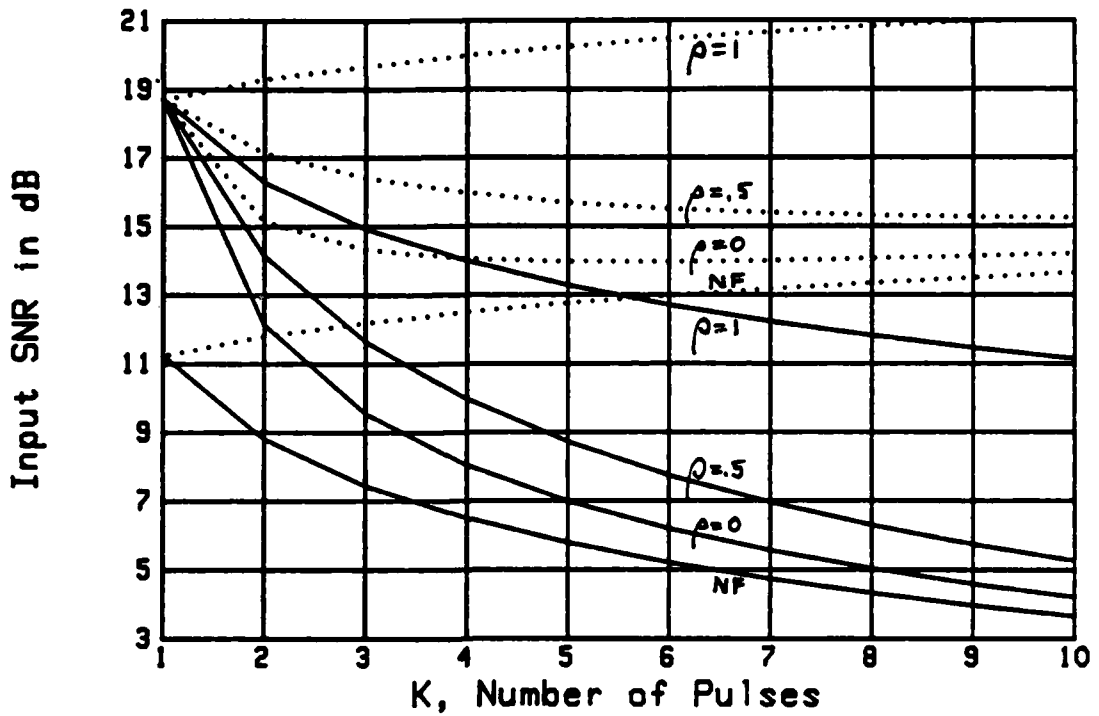


Figure 15.  $P_f = 1E-6$ ,  $P_D = .5$ ,  $m = .25$

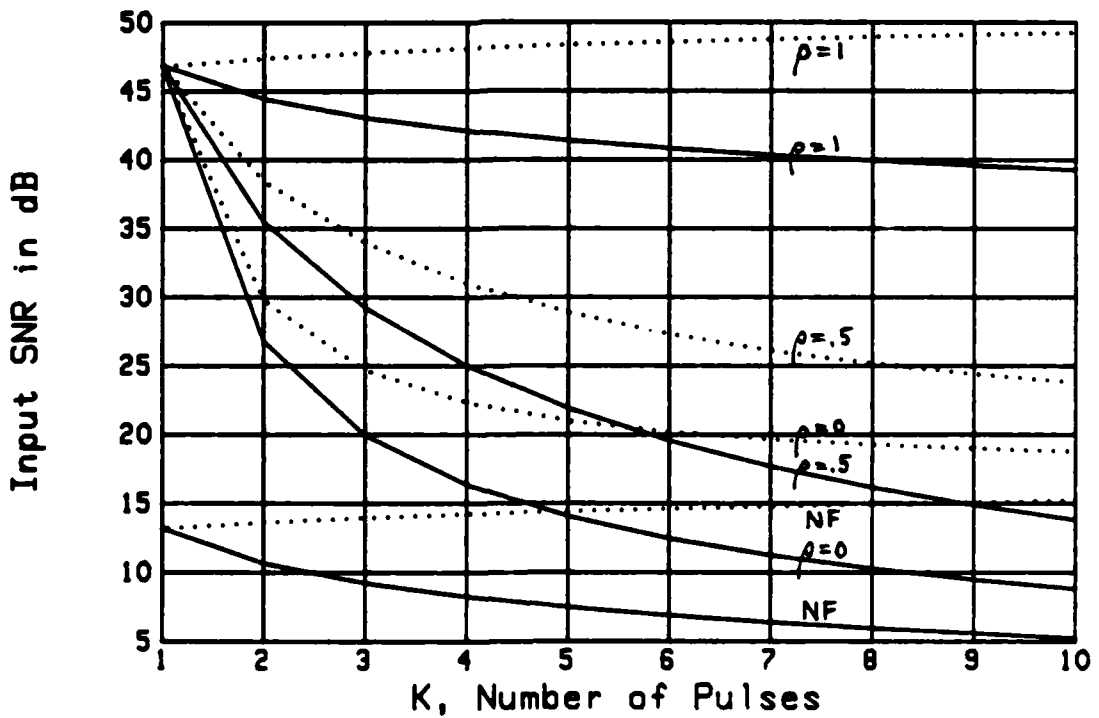


Figure 16.  $P_f = 1E-6$ ,  $P_D = .9$ ,  $m = .25$

TR 7707

## SUMMARY

One manner of summarizing the behavior of the amplitude and power scaling variates (figure 2) is to observe that as the parameter  $m$  decreases from infinity (the nonfading case), the fading becomes deeper more often. For small  $m$ , the very deep fades occur very often. As  $m$  nears zero, the fades are so deep and occur so often that large arguments of the scaling probability density functions are rarely observed. Thus, for a given level of performance, the required input signal-to-noise ratio must increase as  $m$  decreases.

This conclusion is borne out by the  $P_D = .9$ ,  $P_F = 1E-6$  case (figures 4, 8, 12, and 16) where, for a single pulse system,  $K=1$ , the required input signal-to-noise ratio increases from 17 dB to 47 dB as  $m$  decreases from 2 to .25. Relaxing the probability of detection to  $P_D = .5$  relaxes the corresponding signal-to-noise ratios to the range from 12 dB to 19 dB. It is also not surprising that tightening the probability of false alarm to  $1E-8$  further increases the required signal-to-noise ratio. For  $m = .25$  and  $P_F = 1E-8$ , the signal-to-noise ratio requirements are preposterous and the corresponding figures for  $P_D = .5$  and  $P_D = .9$ , which would have completed the set, have been omitted.

Although the signal model employed here in (1) and (4) utilizes a common carrier frequency  $f_0$  for all  $K$  pulses, the results extend immediately to the case of arbitrary different carrier frequencies  $f_k$  for the  $k$ -th pulse.

provided that these various frequencies are known and appropriately used at the receiver. Also, although the particular signal pulse in (1) is a simple burst of a sinewave, the current results extend to arbitrary signal waveforms  $p_k(t)$  on each pulse, provided that matched filters are employed in the receiver, and that each waveform  $p_k(t)$  have identical transmitted energy.

APPENDIX A  
CHARACTERISTIC FUNCTION OF SYSTEM OUTPUT

Matched Filter Output Characterization

In this appendix, we compute the characteristic function of the decision variable, described in (7) et seq. The in-phase and quadrature outputs of the k-th matched filter, at the time instant of peak signal output, are

$$\begin{aligned} \begin{Bmatrix} I_k \\ Q_k \end{Bmatrix} &= \int_L dt \left[ A r_k \cos(2\pi f_0(t - t_k - D) + \theta_k) + n(t) \right] * \\ &* \begin{Bmatrix} \cos \\ \sin \end{Bmatrix} (2\pi f_0(t - t_k - D)) \quad \text{for } 1 \leq k \leq K. \end{aligned} \quad (\text{A-1})$$

where use has been made of (1) and (7), and phase shift  $\theta_0$  has been absorbed in random phase shift  $\theta_k$ , with no loss of generality. That is,

$$I_k = \alpha_k + \mu_k, \quad Q_k = \beta_k + \nu_k, \quad (\text{A-2})$$

where the signal components are, upon use of the facts that  $Lf_0 \gg 1$  and that there is no overlap, as indicated in (3),

$$\begin{aligned} \alpha_k &= \frac{1}{2}AL r_k \cos \theta_k, \\ \beta_k &= -\frac{1}{2}AL r_k \sin \theta_k, \end{aligned} \quad (\text{A-3})$$

and the noise components are

$$\begin{Bmatrix} \mu_k \\ \nu_k \end{Bmatrix} = \int_L dt n(t) \begin{Bmatrix} \cos \\ \sin \end{Bmatrix} (2\pi f_0(t - t_k - D)). \quad (\text{A-4})$$

The noise components in (A-4) are Gaussian zero-mean random variables since

$$\overline{n(t)} = 0, \quad \overline{n(t_1)n(t_2)} = N_d \delta(t_1 - t_2). \quad (\text{A-5})$$

There also immediately follows by the use of (A-5),

$$\overline{\mu_k^2} = \overline{v_k^2} = N_d L \frac{1}{2} \equiv \sigma_n^2, \quad \overline{\mu_k v_k} = 0. \quad (\text{A-6})$$

Furthermore, due to the lack of overlap, as in (3), the random variables  $\mu_k, v_k$  are independent of  $\mu_j, v_j$  for  $k \neq j$ . Thus, the collection of  $2K$  random variables in (A-4) are all independent and identically distributed.

#### Conditional Characteristic Function

The  $k$ -th squared envelope sample at the matched filter output is

$$\gamma_k = I_k^2 + Q_k^2 = (\alpha_k + \mu_k)^2 + (\beta_k + v_k)^2, \quad (\text{A-7})$$

by reference to (A-1) and (A-2). We will temporarily consider that the signal components in (A-3) are fixed non-random constants; then the conditional characteristic function of random variable  $\gamma_k$  is, upon use of (A-6),

$$\begin{aligned} f_k(\xi) &= \overline{\exp(i\xi\gamma_k)} = \overline{\exp[i\xi(\alpha_k + \mu_k)^2 + i\xi(\beta_k + v_k)^2]} = \\ &= \iint d\mu \, dv \frac{1}{2\pi\sigma_n^2} \exp\left(-\frac{\mu^2 + v^2}{2\sigma_n^2}\right) \exp[i\xi(\alpha_k + \mu)^2 + i\xi(\beta_k + v)^2]. \quad (\text{A-8}) \end{aligned}$$

Now let

$$\mu = \rho \cos \theta, \quad v = \rho \sin \theta, \quad (\text{A-9})$$

to get

$$\begin{aligned}
 f_k(\xi) &= \int_0^{\infty} d\rho \rho \int_{-\pi}^{\pi} d\theta \frac{1}{2\pi\sigma_n^2} \exp\left[-\frac{\rho^2}{2\sigma_n^2} + i\xi\{\alpha_k^2 + \beta_k^2 + 2\rho(\alpha_k \cos \theta + \beta_k \sin \theta) + \rho^2\}\right] \\
 &= \exp[i\xi(\alpha_k^2 + \beta_k^2)] \int_0^{\infty} d\rho \frac{\rho}{\sigma_n^2} \exp\left[-\frac{\rho^2}{2\sigma_n^2} + i\xi\rho^2\right] J_0(\xi 2\rho(\alpha_k^2 + \beta_k^2)^{1/2}) = \\
 &= (1 - i\xi 2\sigma_n^2)^{-1} \exp\left[\frac{i\xi(\alpha_k^2 + \beta_k^2)}{1 - i\xi 2\sigma_n^2}\right]. \tag{A-10}
 \end{aligned}$$

Here we employed [3; 8.411 1 and 6.631 4].

The output of the system is the sum of the squared envelope samples in

(A-7):

$$\gamma = \sum_{k=1}^K \gamma_k = \sum_{k=1}^K (I_k^2 + Q_k^2). \tag{A-11}$$

Since all the noise random variables in (A-4) are independent, the conditional characteristic function of system output random variable  $\gamma$  follows from (A-10)

as

$$f_Y^{(c)}(\xi) = (1 - i\xi 2\sigma_n^2)^{-K} \exp\left[\frac{i\xi}{1 - i\xi 2\sigma_n^2} \sum_{k=1}^K (\alpha_k^2 + \beta_k^2)\right]. \tag{A-12}$$

If we now use (A-3), this can be expressed as

$$f_Y^{(c)}(\xi) = (1 - i\xi 2\sigma_n^2)^{-K} \exp\left[\frac{i\xi}{1 - i\xi 2\sigma_n^2} \left(\frac{AL}{2}\right)^2 \sum_{k=1}^K r_k^2\right]. \tag{A-13}$$

It is important to observe that this conditional characteristic function depends on the signal amplitude scalings  $\{r_k\}$  in (4) and (7) only through the sum of squares

$$S = \sum_{k=1}^K r_k^2 = \sum_{k=1}^K q_k, \quad (\text{A-14})$$

where

$$q_k = r_k^2 = \text{power scaling of } k\text{-th pulse}. \quad (\text{A-15})$$

### First Order Statistics of Scalings

Let the first order probability density function of amplitude scaling  $r_k$  in (4) be

$$p_r(u) = \frac{2 u^{2m-1} \exp(-u^2/\alpha)}{\Gamma(m) \alpha^m} \quad \text{for } u > 0 \quad (m > 0), \quad (\text{A-16})$$

where  $m$  need not be an integer. (As an example, for  $m = 1$ ,

$$p_r(u) = \frac{2}{\alpha} u \exp(-u^2/\alpha) \quad \text{for } u > 0, \quad (\text{A-17})$$

which corresponds to Rayleigh amplitude fading.)

The corresponding probability density function for power scaling  $q_k$  in (A-15) is

$$p_q(u) = \frac{u^{m-1} \exp(-u/\alpha)}{\Gamma(m) \alpha^m} \quad \text{for } u > 0 \quad (m > 0). \quad (\text{A-18})$$

This is recognized as the probability density function of a chi-squared random variate with  $2m$  degrees of freedom; however,  $2m$  need not be an integer here.

The general  $\nu$ -th moment of  $q_k$  is

$$\overline{q_k^\nu} = \alpha^\nu \frac{\Gamma(m + \nu)}{\Gamma(m)}, \quad (\text{A-19})$$

and, in particular, we have

$$\bar{q} = \alpha m, \quad \text{Var}(q) = \alpha^2 m, \quad \frac{\text{Std Dev}(q)}{\bar{q}} = \frac{1}{\sqrt{m}}. \quad (\text{A-20})$$

The first order characteristic function of power scaling  $q_k$  is given by the Fourier transform of (A-18):

$$f_q(\xi) = \int du \exp(i\xi u) p_q(u) = (1 - i\xi\alpha)^{-m}. \quad (\text{A-21})$$

#### First Order Characteristic Function of Sum S in Special Cases

If all the power scalings  $\{q_k\}$  in sum S in (A-14) were independent, then the characteristic function of S would be given by

$$(1 - i\xi\alpha)^{-mK}, \quad (\text{A-22})$$

as may be seen from (A-21). This situation could come about approximately when the signal pulses in (2), (4), and (7) are widely separated in time and subject to uncorrelated (linearly independent) fading.

On the other hand, if all the power scalings were completely dependent, then the characteristic function of sum S would be

$$(1 - i\beta\alpha K)^{-m} \quad (A-23)$$

since  $S = Kq_1$  in this case; see (A-14) and (A-21). This case corresponds to close signal pulses and/or very slow fading.

#### Approximate First Order Characteristic Function of Sum S

The latter two results suggest the following form\* as an approximation to the characteristic function of sum S in (A-14) when the power scalings  $\{q_k\}$  are partially dependent:

$$f_S(\beta) \approx (1 - i\beta B)^{-mK_e} \quad (A-24)$$

This latter form of characteristic function has mean  $mK_e\beta$  and variance  $mK_e\beta^2$ . We will choose the two unknown parameters in (A-24) so that these two statistics identically equal the corresponding exact values determined directly from (A-14). Specifically, using (A-20), mean

$$\bar{S} = K \bar{q} = K \alpha m, \quad (A-25)$$

---

\*A similar procedure was employed with great success for a spectral analysis technique in [4; (38) et seq.].

and variance

$$\begin{aligned} \text{Var}(S) &= \overline{(S - \bar{S})^2} = \overline{\left[ \sum_{k=1}^K (q_k - \bar{q}) \right]^2} = \\ &= \alpha_q^2 \sum_{k,\ell=1}^K \rho_{k\ell} = \alpha_q^2 m \sum_{k,\ell=1}^K \rho_{k\ell} , \end{aligned} \quad (\text{A-26})$$

where

$$\rho_{k\ell} = \frac{1}{\alpha_q^2} \overline{(q_k - \bar{q})(q_\ell - \bar{q})} \quad (\text{A-27})$$

is the normalized covariance coefficient of power scalings  $\{q_k\}$ . Combining these quantities, we find that

$$\begin{aligned} K_e &= \frac{K^2}{\sum_{k,\ell=1}^K \rho_{k\ell}} , \\ \beta &= \alpha \frac{K}{K_e} = \frac{\bar{q}}{m} \frac{K}{K_e} . \end{aligned} \quad (\text{A-28})$$

The quantity  $K_e$  in (A-24) and (A-28) can be interpreted as an effective number of independent scalings in (A-14). For example, if  $\rho_{k\ell} = 0$  for  $k \neq \ell$ , then  $K_e = K$ ; while if  $\rho_{k\ell} = 1$  for all  $k, \ell$ , then  $K_e = 1$ . Both of these situations agree with physical intuition. Also, from (A-28),  $\beta = \alpha$  in the former case, and  $\beta = \alpha K$  in the latter case; (A-24) then reduces to (A-22) and (A-23), respectively, as required.

No specific time separations  $\{t_k\}$ , in (4) and (7), need be assumed for (A-28) to apply. Some of the pulses can be close together, while others can be widely separated, subject of course to limitation (3). The only way that the statistical dependencies of the power scalings  $\{q_k\}$  in sum S enter the characteristic function of S is through the double summation of covariance coefficients in (A-28).

#### Unconditional Characteristic Function of Output $\gamma$

The first order probability density function corresponding to characteristic function (A-24) is

$$p_S(u) = \frac{u^{N-1} \exp(-u/\beta)}{\Gamma(N) \beta^N} \quad \text{for } u > 0, \quad (\text{A-29})$$

where

$$N = m K_e. \quad (\text{A-30})$$

None of the parameters,  $N$ ,  $m$ ,  $K_e$ , need be integer. Also,  $N$  can be larger or smaller than  $K$ , the number of signal pulses.

The conditional characteristic function of system output  $\gamma$  was given in (A-13). The unconditional characteristic function of  $\gamma$  is obtained by averaging (A-13) with respect to (A-29):

$$\begin{aligned}
 f_Y(\gamma) &= \int_0^{\infty} du \frac{u^{N-1} \exp(-u/B)}{\Gamma(N) B^N} (1 - i\beta^2 \sigma_n^2)^{-K} \exp \left[ \frac{i\beta}{1 - i\beta^2 \sigma_n^2} \left( \frac{AL}{2} \right)^2 u \right] = \\
 &= (1 - i\beta^2 \sigma_n^2)^{N-K} (1 - i\beta^2 \sigma_T^2)^{-N}, \quad (A-31)
 \end{aligned}$$

where

$$\sigma_T^2 = \sigma_n^2 \left( 1 + \frac{\overline{E_1}}{N_0} \frac{K}{N} \right). \quad (A-32)$$

To obtain this last relation, we used (A-6), (A-28), (A-30), (6), and

$$N_0 = 2N_d, \quad (A-33)$$

the single-sided noise density level stated just above (7).

Equation (A-31) is a compact simple expression for the characteristic function of decision variable  $\gamma$ . It could be used directly in the efficient procedures of [5] to get the cumulative and/or exceedance distributions of  $\gamma$ . In the next appendix, we derive analytic expressions for these probabilities.

TR 7707

## APPENDIX B

## EXCEEDANCE DISTRIBUTION OF SYSTEM OUTPUT

The characteristic function of decision variable  $\gamma$  is given in (A-31). In order to find the corresponding exceedance distribution function, we use the procedure in [6; appendix A]: since we know the characteristic function-probability density function pair

$$\frac{1}{(1 - i\eta a)^J} \leftrightarrow \frac{u^{J-1} \exp(-u/a)}{\Gamma(J) a^J} \quad \text{for } u > 0, \quad (J > 0), \quad (B-1)$$

the probability density function corresponding to multiplicative characteristic function (A-31) is given by convolution

$$p_\gamma(u) = \int_0^u dx \frac{x^{J-1} \exp(-x/a)}{\Gamma(J) a^J} \frac{(u-x)^{N-1} \exp(-(u-x)/b)}{\Gamma(N) b^N} \quad \text{for } u > 0, \quad (B-2)$$

where

$$J = K - N, \quad a = 2\sigma_n^2, \quad b = 2\sigma_T^2. \quad (B-3)$$

We presume  $N < K$  for now, in order that  $J > 0$ .

Employing [3; 3.383 1 and 8.384 1], (B-2) becomes

$$p_\gamma(u) = \frac{\exp(-u/a) u^{K-1}}{a^{K-N} b^N \Gamma(K)} {}_1F_1\left(N; K; u\left(\frac{1}{a} - \frac{1}{b}\right)\right) \quad \text{for } u > 0. \quad (B-4)$$

Since (A-31) is an analytic function of  $N$ , as is its transform (B-4), we can now analytically continue (B-4) to values of  $N \geq K$ .

The exceedance distribution function of  $\gamma$  is

$$\begin{aligned} \text{Prob}(\gamma > u) = Q_Y(u) &= \int_u^{\infty} dx p_Y(x) = \\ &= \frac{1}{\Gamma(K) (b/a)^N} \int_{u/a}^{\infty} dt e^{-t} t^{K-1} {}_1F_1\left(N; K; \frac{b-a}{b} t\right). \end{aligned} \quad (B-5)$$

Reference to (B-3) and (A-32) yields

$$Q_Y(u) = \frac{1}{\Gamma(K) (1+R)^N} \int_{\mathcal{L}}^{\infty} dt e^{-t} t^{K-1} {}_1F_1\left(N; K; \frac{R}{1+R} t\right), \quad (B-6)$$

where

$$R = \frac{\overline{E_1}}{N_0} \frac{K}{N}, \quad \mathcal{L} = \frac{u}{2\sigma_n^2}. \quad (B-7)$$

By expanding  ${}_1F_1$  in a power series according to [3; 9.210 1], integrating term by term, and using the partial exponential [1; 6.5.11]

$$e_j(x) = \sum_{n=0}^j x^n/n!, \quad (B-8)$$

(B-6) develops into the form

$$Q_Y(u) = \frac{\exp(-\mathcal{L})}{(1+R)^N} \sum_{n=0}^{\infty} \frac{\binom{N}{n}}{n!} \left(\frac{R}{1+R}\right)^n e_{K-1+n}(\mathcal{L}). \quad (B-9)$$

This series for the exceedance distribution function converges for all  $R$ , but rather slowly for large  $R$ .

For signal present, (B-9) gives the detection probability. When signal is absent,  $R = 0$  from (B-7), and (B-9) reduces to the false alarm probability

$$P_F = \exp(-\lambda) e_{K-1}(\lambda), \quad (\text{B-10})$$

which is independent of  $N$  (defined in (A-30) and (A-28)).

An alternative form to (B-9) is available if we employ Kummer's transformation [1; 13.1.27] in (B-6):

$$Q_Y(u) = \exp\left(\frac{-\lambda}{1+R}\right) (1+R)^{K-N} \sum_{n=0}^{\infty} \frac{(K-N)_n}{n!} (-R)^n e_{K-1+n}\left(\frac{\lambda}{1+R}\right). \quad (\text{B-11})$$

If  $N$  is an integer and if  $N \geq K$ , this series terminates, and is composed of all positive terms, which makes it very attractive. However, if either condition is violated, then (B-11) converges only for  $R < 1$ , but diverges for  $R > 1$ . Since this latter case is of practical significance, (B-11) is then not too useful for general values of  $N$ .

The only convergence factor in (B-9) is the  $R/(1+R)$  term. However, we can create another convergence term by adding and subtracting  $\exp(\lambda)$  from the partial exponential, since this is its limit value as  $n$  tends to infinity; see (B-8). By then employing the result that [3; 9.100 and 9.121 1]

$$\sum_{n=0}^{\infty} \frac{(N)_n}{n!} \left(\frac{R}{1+R}\right)^n = {}_2F_1\left(N, \beta; \beta; \frac{R}{1+R}\right) = (1+R)^N, \quad (\text{B-12})$$

(B-9) becomes

$$Q_Y(u) = 1 - \frac{\exp(-\mathcal{L})}{(1+R)^N} \sum_{n=0}^{\infty} \frac{\binom{N}{n}}{n!} \left(\frac{R}{1+R}\right)^n \left[\exp(\mathcal{L}) - e_{K-1+n}(\mathcal{L})\right]. \quad (\text{B-13})$$

This last form was used for all the numerical results obtained here; a program for this expansion is given in appendix C. If necessary, a more elaborate and accurate procedure involving only positive summations is developed in [6; pages A-6 to A-8].

To summarize, the parameters required in detection probability (B-13) are

$$\mathcal{L} = \frac{u}{2\sigma_n^2}, \quad R = \frac{\overline{E}_1}{N_0} \frac{K}{N}. \quad (\text{B-14})$$

where  $\sigma_n^2$  is given by (A-6) and  $N$  is given by (A-30) and (A-28). Since  $\mathcal{L}$  is simply a scaled version of  $u$ , we can equally well keep  $\mathcal{L}$  as the fundamental threshold variable in (B-10) and (B-13).

APPENDIX C  
PROGRAM LISTINGS

Two programs are listed here, the first for fading, the second for no-fading, of the received signal. Inputs required of the user for the fading case are given in lines 20 - 50:

Pf    probability of false alarm  
 Pd    probability of detection  
 M    parameter m in (11) and (13)  
 Rho    $\rho_{kl} = \rho^{|k-l|}$  in (10) and (15) .

The particular exponential normalized covariance  $\rho_{kl}$  programmed in line 1490 can be easily replaced by other more general cases of interest to the user.

The output of the main program, line 290, is the value in dB of  $\bar{E}_1/N_0$  in (9), namely a measure of the required system input signal-to-noise ratio to achieve the desired false alarm and detection probabilities. The number of pulses, K, is taken to be 1 to 10 in line 120, but can be easily changed. The first inverse function subroutine in line 770 solves for the required threshold for specified  $P_f$  and K. The second subroutine in line 1130 solves for the required  $\bar{E}_1/N_0$  for specified  $P_D$  and N.

A similar explanation holds for the no-fading program listed at the end of the appendix. Duplicate routines are not listed in full, in order to save space. The word DOUBLE denotes INTEGER variables in Hewlett Packard BASIC on the 9000 computer.

```

10  ! SNR-FADING
20  Pf=1.E-6           ! FALSE ALARM PROBABILITY
30  Pd=.5             ! DETECTION PROBABILITY
40  M=1.             ! FADING PARAMETER (SINGLE PULSE)
50  Rho=.5           ! FADING CORRELATION COEFFICIENT
60  A$="1E-6,.5,1.,.5" ! Pf,Pd,M,Rho
70  Ef=1.E-20        ! TOLERANCE ON Pf
80  Ed=1.E-15        ! TOLERANCE ON Pd
90  DIM Einodb(1:10) ! REQUIRED INPUT SNR PER PULSE (DB)
100 COM DOUBLE K,REAL N,Thr
110 DOUBLE Ks,Ls
120 FOR K=1 TO 10     ! NUMBER OF PULSES
130   S=0.
140   FOR Ks=1 TO K
150   FOR Ls=1 TO K
160   S=S+FNCounorm(Ks,Ls,Rho)
170   NEXT Ls
180   NEXT Ks
190   Keff=K*K/S
200   N=M*Keff
210   Thrinc=1.       ! THRESHOLD INCREMENT
220   Thrstart=-LOG(Pf)-Thrinc ! THRESHOLD STARTING VALUE
230   CALL Inversfunction1(-Pf,Ef,Thrstart,Thrinc,Thr)
240   Einostart=10.   ! E1/No STARTING VALUE
250   Einoinc=1.     ! E1/No INCREMENT
260   CALL Inversfunction2(Pd,Ed,Einostart,Einoinc,Eino)
270   Einodb(K)=10.*LGT(Eino)
280   NEXT K
290   PRINT Einodb(*)
300   CREATE DATA A$,4
310   ASSIGN #1 TO A$
320   PRINT #1;Einodb(*)
330   ASSIGN #1 TO *
340   END
350   !
360   DEF FNPF(Thr)   ! FALSE ALARM PROBABILITY
370   COM DOUBLE K
380   DOUBLE Ks
390   S=T=EXP(-Thr)
400   FOR Ks=1 TO K-1
410   T=T+Thr/Ks
420   S=S+T
430   NEXT Ks
440   RETURN -S      ! - TO YIELD INCREASING FUNCTION
450   FNEED
460   !

```

```

470 DEF FNPd(E1no) ! FADING DETECTION PROBABILITY
480 COM DOUBLE K,REAL N,Thr
490 Error=1.E-10
500 DOUBLE K1,Ks
510 R=E1no*K/N
520 Et=EXP(Thr)
530 K1=K-1
540 N1=N-1.
550 R1=1.+R
560 Q=R/R1
570 E=Te=1.
580 FOR Ks=1 TO K1
590 Te=Te*Thr/Ks
600 E=E+Te
610 NEXT Ks
620 S=B=MAX(Et-E,0.)
630 T=1.
640 FOR Ks=1 TO 1000
650 Te=Te*Thr/(K1+Ks)
660 B=MAX(B-Te,0.)
670 T=T*Q*(N1+Ks)/Ks
680 Pr=T*B
690 S=S+Pr
700 IF ABS(Pr)<=Error*ABS(S) THEN 730
710 NEXT Ks
720 PRINT "1000 TERMS AT: ";K;N;Thr;E1no;Pr/S
730 Pd=1.-EXP(-Thr-N*LOG(R1))*S
740 RETURN Pd
750 FNEND
760 !
770 SUB Inversfunction1(Desired,Error,X1,De1,X2)
780 X2=X1+De1
790 F1=FNPf(X1)
800 F2=FNPf(X2)
810 IF F2>=Desired THEN 860
820 X1=X2
830 X2=X2+De1
840 F1=F2
850 GOTO 800
860 IF F1<=Desired THEN 920
870 X2=X1
880 X1=X1-De1
890 F2=F1
900 F1=FNPf(X1)
910 GOTO 860
920 Xa=X1
930 Xb=X2
940 IF F2-Desired<Desired-F1 THEN 1010
950 T=X1
960 X1=X2
970 X2=T
980 T=F1
990 F1=F2
1000 F2=T

```

```

1010 IF ABS(F2-Desired)<Error THEN 1110
1020 IF F2=F1 THEN 1110
1030 T=(X1*(F2-Desired)-X2*(F1-Desired))/(F2-F1)
1040 T=MAX(T,Xa)
1050 T=MIN(T,Xb)
1060 X1=X2
1070 X2=T
1080 F1=F2
1090 F2=FNPf(X2)
1100 GOTO 1010
1110 SUBEND
1120 !
1130 SUB Inversfunction2(Desired,Error,X1,De1,X2)
1140 X2=X1+De1
1150 F1=FNPd(X1)
1160 F2=FNPd(X2)
1170 IF F2>=Desired THEN 1220
1180 X1=X2
1190 X2=X2+De1
1200 F1=F2
1210 GOTO 1160
1220 IF F1<=Desired THEN 1280
1230 X2=X1
1240 X1=X1-De1
1250 F2=F1
1260 F1=FNPd(X1)
1270 GOTO 1220
1280 Xa=X1
1290 Xb=X2
1300 IF F2-Desired<Desired-F1 THEN 1370
1310 T=X1
1320 X1=X2
1330 X2=T
1340 T=F1
1350 F1=F2
1360 F2=T
1370 IF ABS(F2-Desired)<Error THEN 1470
1380 IF F2=F1 THEN 1470
1390 T=(X1*(F2-Desired)-X2*(F1-Desired))/(F2-F1)
1400 T=MAX(T,Xa)
1410 T=MIN(T,Xb)
1420 X1=X2
1430 X2=T
1440 F1=F2
1450 F2=FNPd(X2)
1460 GOTO 1370
1470 SUBEND
1480 !
1490 DEF FNCounorm(DOUBLE Ka,Ls,REAL Rho)
1500 RETURN Rho/ABS(Ka-Ls)
1510 FNEND

```

```

10  ! SNR-NO-FADING
20  Pf=1.E-6           ! FALSE ALARM PROBABILITY
30  Pd=.5             ! DETECTION PROBABILITY
40  A$="1E-6,.5"     ! Pf,Pd
50  Ef=1.E-20        ! TOLERANCE ON Pf
60  Ed=1.E-15        ! TOLERANCE ON Pd
70  DIM Elnodb(1:10) ! REQUIRED INPUT SNR PER PULSE (DB)
80  COM DOUBLE K,REAL Thr2
90  FOR K=1 TO 10     ! NUMBER OF PULSES
100  Thrinc=1.        ! THRESHOLD INCREMENT
110  Thrstart=-LOG(Pf)-Thrinc ! THRESHOLD STARTING VALUE
120  CALL Inversfunction1(-Pf,Ef,Thrstart,Thrinc,Thr)
130  Thr2=SQR(2.*Thr)
140  Elnostart=10.    ! E1/No STARTING VALUE
150  Elnoinc=1.       ! E1/No INCREMENT
160  CALL Inversfunction2(Pd,Ed,Elnostart,Elnoinc,E1no)
170  Elnodb(K)=10.*LGT(E1no)
180  NEXT K
190  PRINT Elnodb(*)
200  CREATE DATA A$,4
210  ASSIGN #1 TO A$
220  PRINT #1;Elnodb(*)
230  ASSIGN #1 TO *
240  END
250  !
260  DEF FNPf(Thr)     ! FALSE ALARM PROBABILITY
270  COM DOUBLE K
280  DOUBLE Ks
290  S=T=EXP(-Thr)
300  FOR Ks=1 TO K-1
310  T=T*Thr/Ks
320  S=S+T
330  NEXT Ks
340  RETURN -S        ! - TO YIELD INCREASING FUNCTION
350  FNEEND
360  !
370  DEF FNPd(E1no)   ! NO-FADING DETECTION PROBABILITY
380  COM DOUBLE K,REAL Thr2
390  Pd=FNQm(K,SQR(2.*K*E1no),Thr2)
400  RETURN Pd
410  FNEEND
420  !

```

Copy available to DTIC does not  
 permit fully legible reproduction

```

430 DEF FNQm(DOUBLE M, REAL A, B) ! Qm(A, B)
440 Error=1.E-17
450 DOUBLE M1, J
460 Q3=.5*A*A
470 Q4=.5*B*B
480 Q5=EXP(-.5*(Q3+Q4))
490 Q6=Q7=Q5
500 M1=M-1
510 FOR J=1 TO M1
520 Q7=Q7*Q4/J
530 Q6=Q6+Q7
540 NEXT J
550 Qm=Q5*Q6
560 FOR J=1 TO 1000
570 Q5=Q5*Q3/J
580 Q7=Q7*Q4/(J+M1)
590 Q6=Q6+Q7
600 Q9=Q5*Q6
610 Qm=Qm+Q9
620 IF Q9<=Error*Qm THEN 650
630 NEXT J
640 PRINT "1000 TERMS IN FNQm(M, A, B) AT "; M; A; B
650 RETURN Qm
660 FNEND
670 !
SUB Inversfunction1(Desired, Error, X1, Del, X2)
! LISTED ABOVE

SUB Inversfunction2(Desired, Error, X1, Del, X2)
! LISTED ABOVE

```

Copy available to DTIC does not  
 permit fully legible reproduction

## REFERENCES

1. Handbook of Mathematical Functions, U. S. Department of Commerce, National Bureau of Standards, Applied Mathematics Series No. 55, U. S. Government Printing Office, June 1964.
2. A. H. Nuttall, Accurate Efficient Evaluation of Cumulative or Exceedance Probability Distributions Directly from Characteristic Functions, NUSC Technical Report 7023, 1 October 1983.
3. I. S. Gradshteyn and I. M. Ryzhik, Table of Integrals, Series, and Products, Academic Press, Inc., New York, 1980.
4. A. H. Nuttall, Probability Distribution of Spectral Estimates Obtained via Overlapped FFT Processing of Windowed Data, NUSC Technical Report 5529, 3 December 1976.
5. A. H. Nuttall, Signal Processing Studies, NUSC Scientific and Engineering Studies, New London, CT, 1985.
6. A. H. Nuttall, Operating Characteristics for Detection of a Fading Signal with K Dependent Fades and D-fold Diversity in M Alternative Locations, NUSC Technical Report 5739, 25 October 1977.

TR 7707

## INITIAL DISTRIBUTION LIST

Addressee	No. of Copies
ASN (RE&S)	1
OUSDR&E (Research and Advanced Technology)	2
DEPUTY USDR&E (Res & Adv Tech)	1
DEPUTY USDR&E (Dir Elect & Phys Sc)	1
ONR, ONR-100, -102, -200, -400, -410, -422, -425AC, -430	8
COMSPAWARSSYSCOM, SPAWAR 05 (W. R. Hunt)	1
CNO, OP-098, OP-941, OP-951, Code 411 (N. Gerr)	4
DIA (DT-2C)	10
NRL, Code 5132 (Dr. P. B. Abraham) Code 5370 (W. Gabriel), Code 5135 (N. Yen) (A. A. Gerlach)	4
USRD	1
NORDA	1
USOC, Code 240, Code 241	2
NAVSUBSUPACNLON	1
NAVOCEANO, Code 02	2
NAVELECSYSCOM, ELEX 03, 310	2
NAVSEASYSYSCOM, SEA-00, -05R, -06F, 630 (E. L. Plummer, CDR E. Graham IV), 63R (C. C. Walker), -92R	8
NAVAIRDEVCEN, Warminster	1
NAVAIRDEVCEN, Key West	1
NOSC, Code 8302, Code 6565 (Library), Code 713 (F. Harris)	3
NAVWPNSCEN	1
NCSC, Code 724	1
NAVCIVENGLAB	1
NAVSWC	1
NAVSURFWPNCEN, Code U31	1
NISC	1
CNET, Code 017	1
CNTT	1
NAVSUBSCOL	1
NAVTRAEQUIPCENT, Technical Library	1
NAVPGSCOL	2
NAVWARCOL	1
NETC	1
APL/UW, SEATTLE	1
ARL/PENN STATE, STATE COLLEGE	1
CENTER FOR NAVAL ANALYSES (ACQUISITION UNIT)	1
DTIC	2
DARPA, Alan Ellinthorpe	1
NOAA/ERL	1
NATIONAL RESEARCH COUNCIL	1
WOODS HOLE OCEANOGRAPHIC INSTITUTION	1
ENGINEERING SOCIETIES LIB, UNITED ENGRG CTR	1
NATIONAL INSTITUTE OF HEALTH	1
ARL, UNIV OF TEXAS	1

## INITIAL DISTRIBUTION LIST

Addressee	No. of Copies
MARINE PHYSICAL LAB, SCRIPPS	1
UNIVERSITY OF CALIFORNIA, SAN DIEGO	1
NAVSURWEACTR	1
DELSI	1
DIRECTOR SACLANT ASW RES CEN	1
COM SPACE & NAV WAR SYS COM	1
COM NAVAL PERSONNEL R&D CENTER	1
COM NAV SUB COLLEGE	1
B-K DYN INC	1
BBN, Arlington, VA (Dr. H. Cox)	1
BBN, Cambridge, MA (H. Gish)	1
BBN, New London, CT (Dr. P. Cable)	1
EWASCTRI	1
MAR, INC, East Lyme, CT	1
HYDROINC (D. Clark)	1
SUMRESCR (M. Henry)	1
ANALTECHNS, N. Stonington, CT	1
ANALTECHNS, New London, CT	1
EDOCORP (J. Vincenzo)	1
TRA CORP., Austin, TX (Dr. T. Leih, J. Wilkinson)	2
TRA CORP., Groton, CT	1
NETS (R. Medeiros)	1
GESY, D. Bates	1
SONALYSTS, Waterford, CT (J. Morris)	1
ORI CO, INC. (G. Assard)	1
HUGHES AIRCRAFT CO. (S. Autrey)	1
MIT (Prof. A. Baggaroer)	1
RAYTHEON CO. (J. Bartram)	1
Dr. Julius Bendat, 833 Moraga Dr, Los Angeles, CA	1
COOLEY LABORATORY (Prof. T. Birdsall)	1
PROMETHEUS, INC. (Dr. James S. Byrnes)	1
BBN INC., New London, CT (Dr. P. Cable)	1
BBN INC., Arlington VA (Dr. H. Cox)	1
BBN INC., Cambridge, MA (H. Gish)	1
ROYAL MILITARY COLLEGE OF CANADA (Prof. Y. T. Chan)	1
UNIV. OF FLORIDA (D. C. Childers)	1
SANDIA NATIONAL LABORATORY (J. Claasen)	1
COGENT SYSTEMS, INC. (J. P. Costas)	1
IBM CORP. (G. Demuth)	1
UNIV. OF STRATHCLYDE, CLASGOW, SCOTLAND (Prof. T. Durrani)	1
ROCKWELL INTERNATIONAL CORP. (L. T. Einstein and Dr. D. F. Elliott)	2
GENERAL ELECTRIC CO. (Dr. M. Fitelson)	1
HONEYWELL, INC. (D. M. Goodfellow, Dr. Murray Simon, W. Hughey)	3
UNIV. OF TECHNOLOGY, LOUGHBOROUGH, LEICESTERSHIRE, ENGLAND (Prof. J. W. R. Griffiths)	1
HARRIS SCIENTIFIC SERVICES (B. Harris)	1

## INITIAL DISTRIBUTION LIST

Addressee	No. of Copies
UNIV OF CALIFORNIA, SAN DIEGO (Prof. C. W. Helstrom)	1
EG&G (Dr. J. Hughen)	1
A&T, INC. (H. Jarvis)	1
BELL COMMUNICATIONS RESEARCH (J. F. Kaiser)	1
UNIV. OF RI (Prof. S. Kay, Prof. L. Scharf, Prof. D. Tufts)	3
MAGNAVOX GOV. & IND. ELEC. CO. (R. Kenefic)	1
DREXEL UNIV. (Prof. Stanislav Kesler)	1
UNIV. OF CT (Prof. C. H. Knapp)	1
APPLIED SEISMIC GROUP (R. Lacoss)	1
ADMIRALTY RESEARCH ESTABLISHMENT, ENGLAND (Dr. L. J. Lloyd)	1
NAVAL SYSTEMS DIV., SIMRAD SUBSEA A/S, NORWAY (E. B. Lunde)	1
DEFENCE RESEARCH ESTAB. ATLANTIC, DARTMOUTH, NOVA SCOTIA CANADA (B. E. Mackey, Library)	1
MARTIN MARIETTA AEROSPACE (S. L. Marple)	1
PSI MARINE SCIENCES (Dr. R. Mellen)	1
Dr. D. Middleton, 127 E. 91st St. NY, NY 10128	1
Dr. P. Mikhalevsky, 803 W. Broad St. Falls Church, VA 22046	1
CANBERRA COLLEGE OF ADV. EDUC., AUSTRALIA 2616 (P. Morgan)	1
NORTHEASTERN UNIV., (Prof. C. L. Nikias)	1
ASTRON RESEARCH & ENGR, (Dr. A. G. Piersol)	1
WESTINGHOUSE ELEC. CORP. (Dr. H. L. Price)	1
M/A-COM GOVT SYSTEMS, (Dr. R. Price)	1
DALHOUSIE UNIV. HALIFAX, NOVA SCOTIA (Dr. B. Ruddick)	1
NATO SACLANT ASW RESEARCH CENTER, LIBRARY, APO NY, NY 09019	1
YALE UNIV. (Prof. M. Schultheiss)	1
NATIONAL RADIO ASTRONOMY OBSERVATORY (F. Schwab)	1
DEFENSE SYSTEMS, INC (Dr. G. S. Sebestyen)	1
DEPT OF OCEAN ENGR. (Dr. R. C. Spindel, Dr. E. Weinstein)	2
NATO SACLANT ASW RESEARCH CENTRE (Dr. E. J. Sullivan)	1
PENN STATE UNIV, APPLIED RESEARCH LAB. (F. W. Symons)	1
NAVAL PG SCHOOL, (Prof. C.W. Therrien)	1
DEFENCE RESEARCH ESTABLISHMENT PACIFIC, VICTORIA, B.C. CANADA VOS 1B0 (Dr. D. J. Thomson)	1
Robert J. Urick, 11701 Berwick Rd, Silver Spring, MD 20904	1
RCA CORP (H. Urkowitz)	1
USEA S.P.A. LA SPEZIA, ITALY (H. Van Asselt)	1
NORDA, Code 345 (R. Wagstaff)	1
TEL-AVIV UNIV. ISRAEL (Prof. E. Weinstein)	1
COAST GUARD ACADEMY (Prof. J. J. Wolcin)	1
SPACE PHYSICS LAB, UNIV OF ALBERTA, EDMONTON, CANADA (K. L. Yeung)	1
UNIV. OF IOWA (Prof. D. H. Youn)	1

END

10-86

DT/C